Accurate Quantum Chemical Calculations

Charles W. Bauschlicher, Jr. and Stephen R. Langhoff
NASA Ames Research Center
Moffett Field, CA 94035

and

Peter R. Taylor
ELORET Institute†
Sunnyvale, CA 94087

† Mailing address: NASA Ames Research Center, Moffett Field, CA 94035

I. INTRODUCTION

An important goal of quantum chemical calculations is to provide an understanding of chemical bonding and molecular electronic structure, and over the last thirty years this has been largely realized. A second goal, the prediction of energy differences to "chemical accuracy" (about 1 kcal/mole), has been much harder to attain. First, the computational resources required to achieve such accuracy are very large, and second, it is not straightforward to demonstrate that an apparently accurate result, in terms of agreement with experiment, does not result from a cancellation of errors. Therefore, in addition to performing very elaborate electronic structure calculations, calibration and the assignment of realistic uncertainties are also required.

Recent advances in electronic structure methodology (1), coupled with the power of vector supercomputers, have made it possible to solve a number of electronic structure problems exactly using the full configuration interaction (FCI) method within a subspace of the complete Hilbert space. These exact results can be used to benchmark approximate techniques that are applicable to a wider range of chemical and physical problems. They thus provide the necessary calibration of existing techniques for electronic structure calculations, and can be used to determine the origins of any deficiencies. In fact, as we shall show, the calibrations indicate that most of the methods for generating many-electron wave functions perform very well, and that a major source of error in even the best calculations arises at a more elementary level, in the selection of the atomic expansion basis sets. In this review we will discuss the use of FCI wave functions to benchmark simpler computational methods, and new approaches to constructing atomic basis sets that substantially reduce the basis set errors while keeping the overall computational effort manageable.

In the following Section we will review briefly the methodology of many-electron quantum chemistry. In Section III we consider in more detail methods for performing FCI calculations, and in Section IV we discuss the application of FCI methods to several three-electron problems in molecular physics. In Section V we describe a number of benchmark applications of FCI wave functions. In Section VI we discuss atomic basis sets and the development of improved methods for handling very large basis sets: these are then applied to a number of chemical and spectroscopic problems in Section VII, to transition metals in Section VIII, and to problems involving

potential energy surfaces in Section IX. Although the experiences described in these sections give considerable grounds for optimism about our general ability to perform accurate calculations, there are several problems that have proved less tractable, at least with current computer resources, and we discuss these and possible solutions in Section X. Our conclusions are given in Section XI.

II. QUANTUM CHEMICAL METHODOLOGY

In the clamped-nucleus Born-Oppenheimer approximation, with neglect of relativistic effects, the molecular Hamiltonian operator in atomic units takes the form

$$\hat{H} = -\frac{1}{2}\sum_{i=1}^{n}\nabla_i^2 - \sum_{A=1}^{N}\sum_{i=1}^{n} Z_A r_{Ai}^{-1} + \sum_{i>j=1}^{n} r_{ij}^{-1} + \sum_{A>B=1}^{N} R_{AB}^{-1} \qquad (1)$$

in the absence of external fields. The terms in Eq. (1) comprise the electron kinetic energy, the nuclear-electron attraction, the electron repulsion, and the nuclear repulsion, respectively. (Relaxing the assumptions of fixed nuclei and non-relativistic motion can be investigated perturbationally, at least for lighter elements, as discussed briefly later.) Our goal is to approximate solutions to the time-independent Schrödinger wave equation

$$\hat{H}\Psi = E\Psi \qquad (2)$$

for this Hamiltonian. Although some limited progress has been made in approaching Eq. (2) by analytical methods (2), this is a very difficult procedure that is not yet suited to the production of chemical results. Instead, most methods make (implicit or explicit) use of basis set expansion techniques: the unknown eigenfunctions of Eq. (2) are expressed in terms of a set of *n-particle basis functions* $\{\Phi\}$. Again, while it is possible to consider rather exotic functional forms for the Φ, involving, say, interelectronic coordinates, by far the most common approach is to construct each Φ using a product of *molecular orbitals* (MOs — one-electron functions) $\{\psi\}$:

$$\Phi_K = \hat{O}\prod_{i=1}^{n}\psi_i \qquad (3)$$

Here a given function Φ_K involves an $n-$fold product of MOs, to which is applied some projection operator or operators $\hat{O}$. As electrons are fermions, the solutions to Eq. (2) will be antisymmetric to particle interchange, and it is usually convenient to incorporate this into the n-particle basis, in which case the Φ will be Slater determinants. The Hamiltonian given in Eq. (1) is also spin-independent and commutes

with all operations in the molecular point group, so that projection operators for particular spin and spatial symmetries could also appear in $\hat{O}$. The Φ obtained in this way are generally referred to as configuration state functions (CSFs).

The molecular orbitals are usually obtained as linear combinations of a *one-particle basis*

$$\psi_i = \sum_\mu \chi_\mu C_{\mu i}. \tag{4}$$

The one-particle basis functions $\{\chi\}$ are often referred to as atomic orbitals (AOs). The MO coefficients $\mathbf{C}$ are obtained by solving an electronic structure problem simpler than that of Eq. (2), such as the independent particle (Hartree-Fock) approximation, or using a multiconfigurational Hartree-Fock approach (1). This has the advantage that these approximations generally provide a rather good estimate of the solutions to Eq. (2) — perhaps 99% of the total energy or more — thus suggesting that an analysis of the many-electron problem and (possibly) computational schemes for attacking it can be formulated around them. Löwdin (3) defined the "correlation energy" as the difference between the exact energy obtained from Eq. (2) and the Hartree-Fock energy, and the term "correlation problem" is widely used to refer to the problem of computing this energy difference.

The most obvious use of the n-particle basis $\{\Phi\}$ in solving Eq. (2) is the linear *configuration interaction* (CI) expansion

$$\Psi = \sum_K \Phi_K c_K. \tag{5}$$

If the one-particle basis is complete, the use of all possible Φ — termed *complete CI* — in Eq. (5) will yield the exact eigenvalue(s) and eigenfunction(s) of Eq. (2). Incidentally, as the use of Eq. (5) corresponds to the variational problem of making the energy stationary with respect to variations of the coefficients c_K, subject to normalization of Ψ, any guess at the c_K will yield an upper bound to the true energy. In practice, of course, a complete one-particle space is infinite, and so the complete CI problem would also be infinite in dimension. If we choose a finite, truncated one-particle space, but approximate Ψ as in Eq. (5) using all the possible n-particle basis functions, we have a *full CI* (FCI) wave function. The FCI wave function can be regarded as the exact solution to a Schrödinger equation projected onto the finite subspace generated by the truncated one-particle basis.

FCI wave functions have many convenient properties, for example, the results are independent of any unitary transformation on the MOs used to construct the n-particle basis, and as the only approximation made in solving Eq. (2) is the truncation of the one-particle basis, we may identify any discrepancies between calculation and experiment as arising from this truncation (assuming the Born-Oppenheimer approximation and neglect of relativity are valid). Hence it would appear that FCI calculations are an ideal approach for solving the correlation problem. The difficulty, of course, is that the factorial dependence of the length of the FCI expansion on the number of electrons correlated and the number of MOs used creates insuperable computational difficulties for most problems of chemical interest. Even by restricting the correlation treatment to a subset of the electrons, by ignoring correlation effects involving $1s$ electrons in first-row systems, for instance, the expansions will usually be impractically long. To obtain the dissociation energy of the N_2 molecule to within 5 kcal/mole of experiment, for example, would require an FCI expansion of some 10^{14} CSFs, correlating only the ten valence electrons. Thus we must develop schemes for truncating *both* the one-particle and n-particle spaces to arrive at computationally feasible wave functions.

A simple way to implement n-particle space truncation is to use the uncorrelated wave function (which as noted above is a very substantial fraction of the exact wave function) to classify terms in the n-particle space. If we consider the Hartree-Fock determinant, for example, we can construct all CSFs in the full n-particle space by successively exciting one, two... electrons from the occupied Hartree-Fock MOs to unoccupied MOs. For cases in which a multiconfigurational zeroth-order wave function is required, the same formal classification can be applied. Since only singly- and doubly-excited CSFs can interact with the zeroth-order wave function via the Hamiltonian in Eq. (1), it is natural to truncate the n-particle expansion at this level, at least as a first approximation. We thus obtain single and double excitations from Hartree-Fock (denoted SDCI) or its multiconfigurational reference analog, multireference CI (MRCI).

Truncated CI methods are only one of the popular approaches to the correlation problem. Coupled-cluster (CC) schemes (4) use a different formal ansatz from Eq. (5), based on an exponential operator

$$\Psi = \exp(T)\Psi_0 \tag{6}$$

Here T comprises excitation operators that again excite one, two... electrons from

MOs occupied in the zeroth-order function Ψ_0 to unoccupied MOs. The use of the exponential operator guarantees that the energy is additively separable, that is, that the energy of two non-interacting systems is the sum of the two separate system energies. This holds for Eq. (6) irrespective of what truncation is applied to T (say, to only single and double excitations). This *size-consistency* property is *not* shared by truncated CI. On the other hand, if Eq. (6) is substituted into the variation principle the resulting equations for the cluster amplitudes (the weights with which the given single, double... excitation terms appear) are too complicated for practical solution, and CC methods instead solve a non-linear, non-variational equation system for the amplitudes. Hence the CC energy is not a variational upper bound.

Another popular approach to the correlation problem is the use of perturbation theory (5). Ψ_0 can be taken as an unperturbed wave function associated with a particular partitioning of the Hamiltonian, perturbed energies and wave functions can then be obtained formally by repeatedly applying the perturbation operator to Ψ_0. Probably the commonest partitioning is the Møller-Plesset scheme (5), which is used where Ψ_0 is the closed-shell or (unrestricted) open-shell Hartree-Fock determinant. Clearly, the perturbation energies have no upper bound properties, but, like the CC results, they are size-consistent.

A particular advantage of the CI approach, as opposed to coupled-cluster or perturbation theoretic techniques, is that it can be readily formulated to handle the case in which Ψ_0 is multiconfigurational in character. Corresponding multireference CC or perturbation theory approaches are much less well developed. As we shall see there are many important chemical applications where a multireference approach is mandatory, and we shall therefore concentrate mainly on the CI method in this article.

The classification of CSFs into single, double... excitations is straightforward and unambiguous for a closed-shell Hartree-Fock reference function. In open-shell or multireference cases there are more possibilities for defining these excited CSFs, some of which interact with the reference space in the lowest order of perturbation theory, and some of which do not. It is very common to exclude the latter excitations. This is termed restricting the wave function to the first-order interacting space (6).

The choice of reference space for MRCI calculations is a complex problem.

First, a multiconfigurational Hartree-Fock (MCSCF) approach must be chosen. Common among these are the generalized valence-bond method (GVB) (7) and the complete active space SCF (CASSCF) method (8). The latter actually involves a full CI calculation in a subspace of the MO space — the *active space*. As a consequence of this full CI, the number of CSFs can become large, and this can create very long CI expansions if all of the CASSCF CSFs are used as reference CSFs. This problem is exacerbated when it becomes necessary to correlate valence electrons in the CI that were excluded from the CASSCF active space. It is very common to *select* reference CSFs, usually by their weight in the CASSCF wave function. Even more elaborate than the use of a CASSCF wave function as the reference space is the *second-order CI*, in which the only restriction on the CSFs is that no more than two electrons occupy orbitals empty in the CASSCF wave function. Such expansions are usually too long for practical calculations, and they seldom produce results different from a CAS reference space MRCI.

When more than one state of a system is to be investigated, it is possible to perform separate MCSCF calculations, followed by MRCI calculations, on each state. This, however, can be a very expensive process, and if transition properties between states are desired, such as transition dipole moments for spectroscopic intensities, the nonorthogonality between the MCSCF orbitals for the different states creates complications. A simple alternative is to perform an MCSCF optimization of a single average energy for all states of interest (9). All states are thereby described using a common set of MOs. Although these MOs are obviously not optimum for any of the states, experience shows this has little effect on the final MRCI results.

In some cases, even the use of severely truncated reference CSF spaces can give rise to an MRCI expansion that is too long for practical calculations. Siegbahn has developed an approximate scheme for handling such cases: the weights of the singly- and doubly-excited CSFs are estimated perturbationally and frozen, then scale factors multiplying the weights of groups of CSFs are optimized in a so-called *contracted CI* (CCI) calculation (10). Such a calculation requires much less effort than the corresponding MRCI calculation, and the results obtained are generally good. It may be possible in some cases to perform a large number of CCI calculations, say, to characterize a potential energy surface, and to scale the results based on MRCI calibration points to improve the accuracy. Another approach to reducing the number of variational parameters in the CI wave function is the *internally*

contracted CI approach (11). Here single and double excitations are made not from individual reference CSFs but from the MCSCF wave function, which is treated as a single term. The configurations of the reference CSFs are held at their MCSCF values, but this restriction can be relaxed if desired. Internal contraction normally produces results similar to the uncontracted MRCI calculation, but at less cost.

As noted briefly above, truncated CI expansions do not produce size-consistent results. Several approaches of varying sophistication have been developed to address this problem. The single-reference Davidson correction (12)

$$\Delta E = E_{corr}(1 - c_0^2) \tag{7}$$

is a simple perturbation theoretic estimate of the energy effects of higher than double excitations. Here E_{corr} is the correlation energy from single and double excitations and c_0 is the coefficient of the Hartree-Fock determinant. Eq. (7) is very often extended heuristically to the multireference case (13) using the form

$$\Delta E = E_{corr}(1 - \sum_R c_R^2). \tag{8}$$

Here E_{corr} is the difference between the MRCI energy and the energy obtained with the reference CSFs, and c_R is the coefficient of reference CSF R in the MRCI wave function. We shall use the notation (+Q) to denote the use of the corrections given by Eq. (7) or Eq. (8). A problem with such approximations is that as there are no useful bounds on the adjusted energy expression some numerical "noise" can be introduced across a large set of calculations (say, for a potential energy surface), while the MRCI values themselves would be much smoother (14). (This "noise" can also be a problem with those MRCI methods that apply selection to *all* CSFs used, rather than just reference CSFs.) A more sophisticated approach to the size-consistency problem is to modify the CI energy expression so that size-consistent results are obtained. The earliest such schemes are the various coupled-electron pair approximations (CEPA) (15), including the linearized coupled-cluster approach of Cizek (16). The single-reference Davidson correction can be viewed as a first approximation to the solution of the linearized CC equations. More recently, Ahlrichs and co-workers introduced the coupled-pair functional (CPF) (17), which has many similarities with the physical reasoning behind the CEPA schemes, and the averaged CPF (ACPF) approach (18) which can be extended to the multireference

case. An advantage of these methods is that it is easier to apply the powerful techniques of analytic derivative theory to cases in which a functional is made stationary (19). The modified CPF (MCPF) approach of Chong and Langhoff (20) is a development of the single-reference CPF method that often gives better results than the original when the single-reference description is a poor approximation.

The wave function that is used to define the reference CSFs is usually the one used to optimize the MO coefficients, but the ultimate accuracy of the MOs clearly derives from the quality of the AO basis chosen at the outset. In the vast majority of current calculations, the AOs are taken as fixed linear combinations of Gaussian-type functions centered on the nuclei, but the number of functions used, the range of angular momenta, etc, all vary widely among different calculations. We shall discuss a number of these aspects in this review, as the one-particle basis set plays a fundamental role in determining the accuracy of a given calculation.

In summary, then, CI approaches to the correlation problem involve a choice of atomic basis set, the optimization of a Hartree-Fock or MCSCF wave function, the selection of CI CSFs (usually by selecting one or more reference CSFs and all single and double excitations from them), and the optimization of the CI wave function. There are two potential sources of error in this prescription — the choices of one-particle and n-particle spaces. It is these sources of error we shall review in depth in the present work.

III. FULL CONFIGURATION INTERACTION METHODS

The use of the full CI (FCI) procedure as an exact test of approximate methods has been a key element in improving the accuracy of calculations, and we therefore consider the evolution of FCI methodology in some detail.

In the earliest CI programs, the Hamiltonian matrix elements were computed individually over a list of CSFs that could be chosen more or less arbitrarily (21). (This approach is commonly referred to as *conventional CI.*) A given Hamiltonian matrix element H_{KL} can be expanded as

$$H_{KL} = \sum_p \sum_q A_{pq}^{KL}(p|h|q) + \sum_p \sum_q \sum_r \sum_s B_{pqrs}^{KL}(pq|rs), \tag{9}$$

in terms of MO one- and two-electron integrals $(p|h|q)$ and $(pq|rs)$ and *coupling coefficients* A and B. The latter depend on the occupation and spin coupling of the MOs $p, q...$ in the CSFs Φ_K and Φ_L. The matrix elements were stored on disk

or tape, and after all the elements had been computed the desired eigenvalues and eigenvectors were extracted in a subsequent step. Clearly, this approach could be used to perform an FCI calculation. However, the factorial increase in length of the CI expansion with number of electrons and orbitals made this possible for only very small calculations, such as the special case of three-electron systems.

The development of the direct CI approach (22) eliminated the requirement for large peripheral storage for the Hamiltonian matrix and greatly reduced the time to compute the eigenvalues and eigenvectors, as much redundant work in the conventional CI approach was eliminated. In direct CI the residual vector

$$\sigma_K = \sum_L H_{KL} c_L \tag{10}$$

is computed from the expression

$$\sigma_K = \sum_L \sum_p \sum_q A_{pq}^{KL}(p|h|q)c_L + \sum_L \sum_p \sum_q \sum_r \sum_s B_{pqrs}^{KL}(pq|rs)c_L, \tag{11}$$

which results from substituting Eq. (9) in Eq. (10). In this way the Hamiltonian matrix elements themselves never appear explicitly. However, in the earliest formulations of direct CI, each problem (that is, closed-shell single reference, doublet, etc) required the development of a new program, as the A and B values in Eq. (11) were derived by hand and coded into the program. The first direct CI program for full CI calculations with more than two electrons was a three-electron FCI program developed by Siegbahn (23). This program was able to handle relatively large one-particle basis sets, but three-electron problems are neither common enough nor representative enough for such a code to provide many benchmarks.

An important development in FCI methodology was Handy's observation (24) that if determinants were used as the n-particle basis functions, rather than CSFs, the Hamiltonian matrix element formulas could be obtained very simply. Specifically, it was possible to create an ordering of the determinants such that for each determinant, a list of all other determinants with which it had a non-zero matrix element could easily be determined. Further, it was easy to evaluate the coupling coefficients A and B in Eq. (11) (the only non-zero values being ± 1) and therefore to compute the matrix elements. While this greatly expanded the range of FCI calculations that could be carried out, the algorithm is essentially scalar in nature and

therefore rather inefficient on modern supercomputers. Nonetheless, this method supplied some important benchmarks, as discussed below.

Like any general direct CI method, the shape-driven graphical unitary group approach (25) can also be used to perform FCI calculations for some cases, but as in Handy's determinantal scheme matrix elements involving higher than double excitations from the reference CSF are processed using scalar algorithms. Like the Handy determinantal scheme, this approach has been used to provide several benchmarks.

A major advance in the efficiency of FCI calculations was introduction of a factorized direct CI algorithm by Siegbahn (26). This involves formulating the FCI calculation as a series of matrix multiplications: an ideal algorithm for exploiting the power of current vector supercomputers. This algorithm is fundamental to our present ability to perform FCI benchmarks and we discuss it in detail. We consider only the two-electron contribution to σ given by Eq. (11), which can be written as

$$\sigma_K = \sum_p \sum_q \sum_r \sum_s \sum_L (pq|rs) B^{KL}_{pqrs} c_L. \tag{12}$$

Siegbahn noted that by inserting a resolution of the identity, B^{KL}_{pqrs} can be factorized explicitly into products of one-electron coupling coefficients:

$$B^{KL}_{pqrs} = \sum_J A^{KJ}_{pq} A^{JL}_{rs}. \tag{13}$$

This approach had been used earlier to compute the coupling coefficients themselves (27); but if instead the factorization of B is inserted into Eq. (12) the calculation of σ can be completely vectorized. First, the product of one set of coupling coefficients and c is collected in $\mathbf{D}$,

$$D^J_{rs} = \sum_L A^{JL}_{rs} c_L. \tag{14}$$

This can be implemented as vector operations; it should be noted that there are very few non-zero A values and this sparseness can be exploited in evaluating Eq. (14). A matrix multiplication of this intermediate matrix $\mathbf{D}$ and a block of the integrals is performed,

$$E^J_{pq} = \sum_{rs} (pq|rs) D^J_{rs}. \tag{15}$$

Finally, the intermediate array **E** is merged with the second set of coupling coefficients to form a contribution to σ,

$$\sigma_K = \sum_J \sum_{pq} A_{pq}^{KJ} E_{pq}^J. \tag{16}$$

All steps in the calculation of σ are vectorizable, and perform well on vector supercomputers. For large basis sets the matrix multiplication step in Eq. (15) will dominate the computational effort.

This factorized direct CI scheme still has some difficulties, however. In particular, values of the coupling coefficients A are required. While the lists of A values are extremely sparse, for very large calculations there will be many non-zero values, which must either be precomputed and stored, or computed on the fly. As Siegbahn's intended application was in generating FCI wave functions for use in CASSCF optimizations, he stored the coupling coefficients on a disk file. For very large calculations disk space becomes the limiting factor, not the CPU power of the computer being used. It is not feasible to perform useful FCI benchmark calculations using this technique in such a form. The modified strategy developed by Knowles and Handy (28) overcame this limitation: these authors showed that by using determinants instead of CSFs, all non-zero A_{pq}^{KL} values (which are ± 1) can be computed almost trivially on the fly. The CI vector is much longer when determinants are used instead of CSFs, but this is not a major handicap when large memory computers such as the CRAY-2 are employed. Thus the factorized, determinantal FCI scheme allows FCI calculations to be performed for very large expansions and hence to be used for benchmarking approximate methods. In essence, the scheme arises from a trade-off between memory (and CPU time) and disk storage: such a trade-off is not an uncommon feature of programming for modern supercomputers.

The most time-consuming step in the Knowles and Handy determinantal FCI scheme, as noted above, is a series of matrix multiplications, so the code performs very efficiently on Cray computers. Calculations as large as 28 000 000 determinants have been performed on the CRAY-2 (29); the **c** and σ vectors and some scratch arrays must be held in memory, so about 60 million words were required. In fact, memory is no longer the resource limitation on current supercomputers, it is disk space that becomes critical. The Davidson diagonalization process (30) used to obtain the lowest eigenvalue(s) and eigenvector(s) requires the **c** and σ vectors from the previous iterations. Therefore, just as storing the coupling coefficients

could exhaust the disk storage long before the CPU time became prohibitive in Siegbahn's factorized scheme, so can the storage of the previous $\mathbf{c}$ and σ vectors in the determinantal algorithm. As Davidson noted in the derivation of his iterative diagonalization algorithm (30), it is possible to fold all the previous vectors into one vector — in effect, the calculation is restarted with a new trial vector corresponding to the best guess available from a fixed number of iterations. While this can slow convergence slightly, it limits the disk storage required. In practice, with the CPU power of, say, the CRAY-2 and the high degree of vectorization in the FCI scheme, as compared to the speed and limits in disk space, it becomes mandatory to use folding of the vectors to make the largest calculations feasible.

Several recent developments should further improve the efficiency of FCI calculations. Olsen *et al.* (31) have derived and implemented a factorized determinantal scheme formulated somewhat differently from that of Knowles and Handy. It appears that the new scheme should be especially efficient for large basis sets and few electrons correlated, which is the situation generally encountered in benchmark calculations. Another development concerns the form of the n-particle basis. Although the use of determinants avoids any storage of coupling coefficients, it generates a longer CI vector than would the use of CSFs and, more importantly, can lead to collapse of an excited state to a lower state of a different spin symmetry due to numerical rounding in the iterative diagonalization (32). This can be a problem, not only in FCI benchmarks, but also in the FCI step in a CASSCF calculation, where one may wish to extract many roots in the study of spectroscopic problems. Recently, Malmqvist *et al.* (33) have proposed a method of using CSFs instead of determinants, but still avoiding the storage of the coupling coefficients on disk. Their approach seems ideal for the CASSCF problem where the number of active orbitals is limited, but may not be suitable for the large FCI calculations used for benchmarking.

It is clear that FCI wave function optimization is currently an active area of research, and the best method of performing FCI calculations may not yet have been achieved. Indeed, in very recent work Knowles (34) has shown how sparseness in $\mathbf{c}$ and σ can be exploited to reduce the computational effort, and Knowles and Handy (35) have been able to perform pilot calculations for a 400 000 000 determinant FCI. Harrison and Zarrabian (36) have modified the factorization used in the original Knowles and Handy scheme so as to reduce the dimension of the interme-

diate space that appears in the resolution of the identity: this approach has been used to perform FCI calculations with over 50 000 000 determinants. It should be feasible to perform calculations with well over 100 000 000 determinants with this approach. Thus it may well become possible to perform even larger benchmarks in the near future. As we will show below, this is important because for some problems there is a coupling of the one- and n-particle spaces, and larger FCI calculations will lead to an improved understanding of a larger range of problems.

IV. FCI APPLICATION CALCULATIONS

The simplest non-trivial FCI calculation is the three-electron case, for which the n-particle problem can be solved exactly for a very large one-particle space. Since relativistic effects, which are neglected, are expected to be very small for the systems considered in this work, the results should be nearly exact, and hence should compare well with experiment. In this section we present three examples where three-electron FCI calculations have yielded accurate results of chemical interest.

The $H_2+H \rightarrow H+H_2$ exchange reaction has been studied by Siegbahn and Liu (37) using the FCI approach in a large one-particle basis set. The potential energy surface for this reaction is estimated to be within 1 kcal/mole of the exact surface, and has been widely used to evaluate scattering methods.

FCI calculations have also been used to assess whether H_2 has a positive electron affinity (EA) (38). The impetus for this study was a qualitative calculation suggesting that H_2 might have a small EA if the "extra" electron attached into the $2\sigma_g$ orbital (39). Before asking experimentalists to investigate this possibility, it seemed worthwhile to carry out FCI calculations in a large basis set, as this requires only a few hours of computer time including convergence tests of the one-particle basis. FCI calculations using a large [5s 4p 3d 1f] Gaussian basis set, which yields an EA of H that is 0.006 eV smaller than the best value and a D_e of H_2 that is only 0.03 eV too small, conclusively shows that H_2 does not have a positive EA. Thus, it is unlikely that a bound state of H_2^- can be observed experimentally.

Another example of a three-electron FCI application is the study of the ^2D Rydberg series in the Al atom (40). The ground state of Al is $^2P(3s^2 3p^1)$. The valence occupation $3s^1 3p^2$ gives rise to a ^2D state, and it was suggested that one of the lowest terms in the $3s^2 nd^1(^2D)$ Rydberg series might correspond to this occupation, although this is contrary to some experimental evidence (41,42). Theoretical

studies indicated some mixing of the $3s^1 3p^2$ configuration into the lower terms of the ^2D Rydberg series (43,44). Further, experimental observations by Garton (41) suggested that a state lying beyond the ionization limit of the ^2D series is derived principally from the $3s^1 3p^2$ occupation. Although this problem is amenable to a CASSCF/MRCI calculation, the FCI calculations eliminate any concern that there is a bias in the treatment of the n-particle space that could lead to an incorrect mixing of occupations. FCI calculations in a [7s 6p 11d 3f] basis set yield excitation energies for the first eight terms in the Rydberg series that are in excellent agreement with experiment. This agreement as well as direct calculation indicates that core-valence correlation has little effect on the term energies, thereby justifying a three-electron treatment. Since this FCI calculation solves the n-particle problem exactly using a large one-particle basis set, and the term energies agree well with experiment, the wave functions should reflect the true configurational mixing in these states. Although a FCI treatment is independent of the orbital basis, we take the d orbitals from the $3s^2(^1S)$ state of Al^+ that corresponds most closely to the Rydberg series to simplify the interpretation. Analysis of the FCI wave function indicates that the percentage contribution of the $3s^1 3p^2$ configuration in the first member of the Rydberg series is 24%. The contribution of $3s^1 3p^2$ rapidly decreases so that the contributions to the fourth and sixth terms are only 6.1% and <1%, respectively. There is 17% of $3s^1 3p^2$ occupation not accounted for in the Rydberg series, which is concentrated in a state just above the IP limit as suggested by experiment. Thus the FCI calculations have definitively resolved the nature of the $3s^1 3p^2(^2D)$ state.

V. FCI BENCHMARK CALCULATIONS

The factorial growth of the FCI treatment with basis set and number of electrons clearly limits its applicability. However, FCI calculations can be performed in moderate-sized (double-zeta plus polarization (DZP) or better) basis sets to calibrate approximate methods of including electron correlation. Thus there is considerable incentive to utilize these FCI methods and the capabilities of modern day supercomputers to perform large-scale benchmark calculations. In this section we consider several examples of the insight obtained from FCI benchmark calculations. In the sections dealing with applications we consider additional FCI benchmark calculations in conjunction with specific applications.

Early FCI benchmark calculations were performed by Handy and co-

workers (45,46). Using a double-zeta (DZ) basis set, they considered stretching the O-H bond lengths in the H_2O molecule to 1.5 and 2.0 times their equilibrium values. The FCI results showed that even the restricted Hartree-Fock (RHF) based fourth-order many-body perturbation theory (MBPT) approach (47,48), which includes the effects of single, double, triple and quadruple excitations, did not accurately describe the stretching of the bond; the error increased from 0.6 kcal/mole at r_e to 10.3 kcal/mole with the bonds stretched to twice their equilibrium values. Although the MBPT method is rigorously size-consistent and contains the effects of higher than double excitations, it does not describe the bond-breaking process well, because the RHF reference becomes a poor zeroth-order description of the system as the bond is stretched. Size-consistent methods that include double excitations iteratively — infinite-order methods such as the coupled-cluster approach — do better. However, only methods that account for the multireference character in the wave function as the bonds are broken, such as the CASSCF/MRCI method, provide an accurate description at all bond lengths (49).

While these earlier studies helped calibrate methods for the approximate treatment of the correlation problem, there were insufficient studies to draw general conclusions about the accuracy of approximate methods. Also, the one-particle basis sets were not large enough to eliminate concerns about possible couplings of the approximations in the one- and n-particle treatments. Much more extensive benchmarking has recently been possible with advances in computers and methods (29,32,50-71). Unlike the earlier work, the basis sets are of at least DZP quality and a sufficient number of systems have been studied that trends are distinguishable. The FCI studies discussed in the remainder of this work use a version of the Knowles and Handy program. As discussed in Section III, this method is based on the work of Siegbahn and vectorizes very well.

The first application of the recent series of benchmarks was the calculation of the total valence correlation energy of Ne atom (50). In this work the FCI was compared to several single-reference-based approaches. These calculations showed that both the +Q correction and the CPF approach gave reasonable estimates for the energy lowering of quadruple excitations, and that the accuracy of the different treatments varied with basis set. The calculations further showed that higher than quadruple excitations were not important in any basis set. It must be remembered that Ne is exceptionally well described by a single reference configuration. It is

clear from the results of the H_2O calculations that to obtain the best possible agreement with the FCI it will be necessary to go beyond the single-reference-based approaches (72). However, the Ne results do suggest that for some problems single-reference-based approaches that include an estimate of higher excitations should yield reasonably accurate results.

To evaluate single-reference and multireference CI approaches to the correlation problem further, we compare in Table I the FCI $^1A_1 - {}^3B_1$ separation in CH_2 with various truncated CI results (53). Since the $^1A_1$ and $^3B_1$ states are derived nominally from the ^3P and ^5S states of carbon, respectively, they involve different bonding mechanisms that result in a substantial correlation contribution to the separation: the SCF separation is over 14 kcal/mole too large. The error of 2.7 kcal/mole at the SDCI level is still much larger than required for chemical accuracy ($\approx$ 1 kcal/mole). The inclusion of the contribution of unlinked higher excitations through either the Davidson correction (+Q) or the CPF method reduces the error substantially. The origin of the error in the SCF/SDCI treatment is the second important configuration, arising from the double excitation $3a_1^2 \rightarrow 1b_1^2$, in the $^1A_1$ state. If the orbitals for the $^1A_1$ state are optimized in a two-configuration SCF calculation, and correlation is included by performing an MRCI calculation based on both these reference configurations, the error is about half that of the SDCI+Q or CPF treatments. The error is reduced to only 0.06 kcal/mole if the multireference analog of the +Q correction is added. After the $3a_1^2 \rightarrow 1b_1^2$ excitation, the next most important correlation effect is that associated with the C-H bonds. If this correlation effect is accounted for in the CASSCF zeroth-order reference for a subsequent MRCI calculation, essentially perfect agreement between the MRCI and FCI is observed. That is, a well-defined CASSCF/MRCI treatment accounts for all of the differential correlation effects. It is interesting to note that adding the multireference +Q correction to this MRCI energy results in overestimating the effect of higher excitations and the separation becomes smaller than the FCI result.

We next consider the spectroscopic constants (59) for the ground state of N_2. The values obtained at various levels of correlation treatment with six valence electrons correlated are summarized in Table II. The SDCI calculation yields a bond length that is in good agreement with the FCI, but the error in D_e is 0.45 eV, even when size-consistency problems are minimized by using the $^7\Sigma_u^+$ state of N_2 to represent two ground state N(^4S) atoms at infinite separation. Although the addition

of quadruple excitations — either variationally (SDQCI) or by the +Q, CPF or MCPF approximations — further reduces the error in D_e, it remains too large for chemical accuracy. If both triple and quadruple excitations are included, the spectroscopic constants are all in good agreement with the FCI. However, this level of treatment is prohibitively expensive in a large one-particle basis set, and even this wave function does not dissociate correctly to ground state atoms, as this requires six-fold excitations relative to the SCF configuration at r_e. The spectroscopic constants computed from an MRCI treatment based on a CASSCF wave function are in excellent agreement with the FCI. Furthermore, this treatment agrees with the FCI for all r values. The addition of the +Q correction does not affect r_e or ω_e, but it makes D_e too large compared with the FCI. A comparison of the computational difficulties encountered in describing the triple bond in N_2 with the single bond in CH_2 confirms that electron-dense systems put a much greater demand on the computational methodology.

In addition to the total energy of the system, it is desirable to carry out FCI calibration studies of properties such as dipole moments, polarizabilities and electrostatic forces. For example, in the $O+OH \rightarrow O_2+H$ reaction (73), the preferred approach of the O atom is determined by the dipole-quadrupole interaction. At long distances this favors a collinear approach to the H atom, whereas for reaction to occur the O atom must migrate to the O end of OH. An accurate description of weakly interacting systems such as van der Waals complexes requires a quantitative description of dipole-induced dipole or induced-dipole induced-dipole interactions. Further, the dipole moment and polarizability functions of a molecule determine its infrared and Raman spectral intensities.

As a first example of an FCI calibration of properties we present in Table III a study of the polarizability of F^- (56). As in the previous examples, the SDCI treatment contains significant error. The inclusion of an estimate of higher excitations improves the results; in this case CPF is superior to the +Q correction. In the multireference case two different approaches were used. In the first, the CASSCF included the $2p$ electrons and the $2p$ and $3p$ orbitals in the active space, and all CASSCF CSFs were used as references for the CI, in which the $2s$ and $2p$ electrons were correlated. Results obtained in this way are denoted MRCI in Table III. A more elaborate CASSCF calculation, with the $2s$ and $2p$ electrons and the $2s$, $3s$, $2p$ and $3p$ orbitals in the active space, was also performed: the use of all

these CASSCF CSFs as references gives results denoted as MRCI′ in Table III. The MRCI and MRCI′ results do not agree as well with the FCI as do the MRCI+Q or MRCI′+Q results. The +Q correction does not overshoot as it did for N_2 and CH_2, in part because of the larger number of electrons correlated here. As noted above, when only six electrons are correlated, the CASSCF/MRCI accounts for such a large percentage of the correlation energy that the +Q correction overestimates the remaining correlation. For more than six electrons, or for cases where the zeroth-order wave function used is less satisfactory than was the CASSCF for N_2 and CH_2, the +Q correction is a better approximation. This is especially true for such quantities as electron affinities that involve large differential correlation effects. Thus the +Q correction substantially improves the agreement with the FCI for the electron affinity of fluorine (29), even when large CASSCF active spaces and MRCI wave functions are employed.

VI. ANO BASIS SETS

In the previous section we showed that the CASSCF/MRCI approach yields results in excellent agreement with FCI, that is, results that are near the n-particle limit. We may therefore expect excellent agreement with experiment when the CASSCF/MRCI approach is used in conjunction with extended one-particle basis sets. It has become clear (74-76) that, until recently, the basis set requirements for achieving the one-particle limit at the correlated level were commonly underestimated, both in the number of functions required to saturate the space for each angular momentum quantum number and in the maximum angular momentum required. For the segmented basis sets that are widely used in quantum chemistry (77), improving the basis set normally involves replacing a smaller primitive basis set with a larger one. It is then seldom possible to guarantee that the smaller basis spans a subspace of the larger set, and it is thus difficult to establish how results obtained with different basis sets relate to convergence of the one-particle space. Ideally, the possibility of differences in primitive basis sets would be eliminated by using a single (nearly complete) primitive set, contracted in different ways such that the smaller contracted sets are subsets of the larger one. Such an approach is best implemented using a general contraction scheme, such as the one proposed by Raffenetti (78) for contracting valence orbitals at the SCF level. However, using

atomic SCF orbitals to define the contraction is not necessarily suitable for handling the correlation problem, and provides no means to contract polarization functions, which require large primitive sets for accurate results. Calculations on molecular systems have shown (79) that natural orbitals (NO) provide an efficient method of truncating the orbital space in correlated treatments. Almlöf and Taylor (80) have proposed an NO procedure for contracting atomic basis sets suitable for use in correlated molecular calculations: this atomic natural orbital (ANO) approach is an efficient method for contracting large primitive valence and polarization basis sets. It has the advantage that the natural orbital occupation numbers provide a criterion for systematically expanding the basis set.

These ideas are illustrated for N atom and N_2 in Table IV. As the contraction of the (13*s* 8*p* 6*d*) primitive set is expanded from [4*s* 3*p* 2*d*] to [5*s* 4*p* 3*d*] to [6*s* 5*p* 4*d*], the correlation energy systematically converges to that of the uncontracted results. The same is true for the (4*f*) and (2*g*) polarization sets. When these ANO sets are applied to N_2, the same systematic convergence of D_e is observed. An additional advantage of the ANO contractions is that the optimum atomic description they provide reduces the problem of *basis set superposition error* (SE) (81,82), in which basis functions on one atom improve the description of another atom, causing a spurious lowering of the computed molecular energy. Superposition error is a particular problem in calculations that aim at high accuracy, and it is highly desirable to minimize its effects.

In order to treat atomic states with different character equally, the ANOs can be averaged to yield a compromise set (83). This is useful for systems with different charges, such as F and F^- or transition metals where the radial expectation values of the 3*d* and 4*s* orbitals are very different for the $3d^n4s^2$, $3d^{n+1}4s^1$ and $3d^{n+2}$ occupations. Generating the average ANOs is analogous to the state averaging used to define compromise orbitals suitable for describing molecular states of different character. A [5*s* 4*p* 3*d* 2*f* 1*g*] contraction based on the average of F and F^- has an SDCI level EA that agrees with the uncontracted (13*s* 9*p* 6*d* 4*f* 2*g*) basis set result to within 0.01 eV. This can be compared with a 0.1 eV error for the same size basis set that is contracted for F alone, but with the outermost (the most diffuse) *s* and *p* primitive functions uncontracted. The results are better if the contraction is based on F^- instead of F, but not as good as using the average ANOs. The loss in total energy as a result of averaging is also very small. ANO basis sets averaged

for different states should thus supply a more uniform description in cases in which there is charge transfer or ionic/covalent mixing. The success for transition metals is equally good: the average ANOs yield separations between the lowest states that are virtually identical to the uncontracted basis set. It should be noted, however, that it may still be necessary to uncontract the most diffuse primitive functions and/or add extra diffuse functions to describe properties such as the dipole moments and polarizabilities (84,85) that are sensitive to the outer regions of the charge density. For example, in Ni atom the polarizability is in excellent agreement with the uncontracted basis set if the outermost s and p functions are uncontacted, but half the uncontracted value if these functions are included in the ANO contraction.

Dunning (86) has recently suggested that accurate results can be obtained with smaller primitive polarization sets than those used in the ANO studies, thereby reducing the integral evaluation time. This approach is consistent with the ANO procedure in that the primitives are optimized at the CI level for the atoms. Since his basis sets contain uncontracted primitive polarization functions and segmented valence sets with the outermost functions free, the basis sets are accurate for properties as well as the energy. For example, Dunning's results for OH are in good agreement with calculations employing ANO sets. However, these conclusions may be system dependent as indicated by the work of Ahlrichs and coworkers on the N_2 (87) and F_2 (74) molecules. Despite optimizing the polarization sets at the CI level for the molecules themselves, the energies for these two homonuclear diatomics did not converge as quickly with expansion of the primitive sets as with ANOs. We conclude that it might be possible to reduce the size of the primitive sets, but this requires more study.

VII. RESULTS FOR SPECTROSCOPIC CONSTANTS

The FCI benchmark calculations discussed in Section V show that a CASSCF/MRCI treatment is capable of accurately reproducing the FCI results, at least when six electrons or fewer are correlated. Further, the ANO basis sets discussed in Section VI show that it is now possible to contract nearly complete primitive sets to manageable size with only a small loss in accuracy. Therefore, a six-electron CASSCF/MRCI treatment performed in a large ANO basis set is expected to reproduce accurately the FCI result in a complete one-particle basis set, and hence should accurately reproduce experiment. For some systems containing

eight electrons, the MRCI agrees well with the FCI, while for others that have very large correlation effects, such as systems with significant negative ion character, it is necessary to include the +Q correction to achieve chemical accuracy. FCI calibration for systems with more than eight electrons have not been possible, but we expect that the +Q correction will improve the results in most cases. In Sections VII-IX we illustrate several calculations that have achieved unprecedented accuracy by combining FCI benchmarks and ANO basis sets.

As discussed previously, FCI calculations for CH_2 show that the CASSCF/MRCI treatment accurately accounts for the differential correlation contribution to the CH_2 $^1A_1 - {}^3B_1$ separation. In Table V, this level of treatment is performed using increasingly accurate ANO basis sets (88). It is interesting to note that although the [4*s* 3*p* 2*d* 1*f*/3*s* 2*p* 1*d*] basis set contains fewer contracted functions than the largest segmented basis sets previously applied to this problem (89), it produces a superior result for the separation. The largest ANO basis set used gives a separation in good agreement with, but smaller than, the T_e value deduced from a combination of theory and experiment (90). From the convergence of the result with expansion of the ANO basis set, it is estimated that the valence limit is about 9.05±0.1 kcal/mole. The remaining discrepancy with experiment is probably mostly due to core-valence correlation effects. However, as the valence correlation treatment is nearly exact, finer effects such as Born-Oppenheimer breakdown (91) and relativity must also be considered. While FCI calculations have shown that a very high level of correlation treatment is required for an accurate estimate of the CV contribution to the separation, theoretical calculations (66) indicate that CV correlation will increase the separation by at most 0.35 kcal/mole — see later discussion. Therefore, it is now possible to achieve an accuracy of considerably better than one kcal/mole in the singlet-triplet separation in methylene.

An analogous study (88) for SiH_2 indicates that the singlet-triplet separation can also be accurately computed for this second-row molecule — see Table V. In fact, the differential valence correlation contribution to T_e converges faster with basis set expansion than for CH_2. Note also that the $^1A_1$ state of SiH_2 is better described by a single reference than is the $^1A_1$ state of CH_2. However, it now becomes necessary to include the dominant relativistic contributions, namely the mass-velocity and Darwin terms (92), via first-order perturbation theory (93) or by using an effective core potential (94), if chemical accuracy is to be achieved. Once relativis-

tic effects and zero-point energy (95) have been accounted for, the theoretical T_0 value of 20.92 kcal/mole is in excellent agreement with the higher experimental value (96). These calculations rule out the alternative value of -18.0 kcal/mole for the $^1A_1 - {}^3B_1$ separation based on a lower value for the ionization potential of the $^1A_1$ state of SiH_2. Thus in addition to establishing the T_e of SiH_2, these calculations also establish the IP of the $^1A_1$ state to be 9.15 eV, the higher of two recent experimental values (see discussion in Ref. 96). We should note that Balasubramanian and McLean (97) independently came to the same conclusion. In their calculations a more conventional segmented one-particle basis set was used and therefore the accuracy of the SiH_2 calculations was not sufficient to definitively determine the T_e value. However, by treating both CH_2 and SiH_2 to about the same accuracy they were able to predict an accurate T_e value for SiH_2 using the error in their CH_2 calculations. The advantage of the ANO basis sets is that they provide a convenient method of systematically approaching the basis set limit. This reduces the need to use an analogous better-known system for calibration. This is advantageous as it can be difficult to find such a system for comparison.

As the calculations on CH_2 and SiH_2 show, theory is now capable of computing energy separations between electronic states to better than a few hundred wavenumbers for both first- and second-row systems. Thus, theory has considerable utility for determining the ground state when two nearly degenerate states are present, which is the case for the Al_2, Si_2 and N_2^{2+} molecules. In the subsequent discussion we describe how FCI benchmark calculations combined with ANO basis sets have allowed a definitive prediction of the ground state for these molecules.

Three possible ground states have been suggested for Al_2 based on previous theoretical calculations (98-101) and experimental studies (102-105). These are the $^3\Sigma_g^-(\pi_u^2)$ and $^3\Pi_u(\sigma_g^1\pi_u^1)$ states with two one-electron bonds and the $^1\Sigma_g^+(\sigma_g^2)$ state with one two-electron bond. All of these states correlate with the $^2P(3p^1)$ ground state of two Al atoms. The accuracy of the CASSCF/MRCI treatment for Al_2 was confirmed using FCI calculations in a small basis set (62). In order to confirm that the one- and n-particle spaces were not strongly coupled, the FCI calibrations were performed in two different one-particle basis sets. For both basis sets the FCI and CASSCF/MRCI T_e values agreed. CASSCF/MRCI calculations (62), including relativistic effects, were then performed in a large ANO basis, showing that the $^3\Pi_u$ state of Al_2 lies just 174 cm^{-1} below the $^3\Sigma_g^-$ state. The $^1\Sigma_g^+$ state was found to

lie much higher in energy. While it is straightforward to carry out CASSCF/MRCI calculations with six valence electrons correlated, even in very large ANO basis sets, it is far more difficult to include the Al $2s$ and $2p$ electrons at this level of correlation treatment. However, the FCI benchmark calculations also showed that the CPF state separations were qualitatively correct. Since the CPF method is size-consistent, it is expected that increasing the number of electrons correlated will not significantly affect its accuracy. It was, therefore, possible to use the CPF approach to show that the L-shell and L-M intershell correlation has little effect on the $A-X$ separation, although it shortens the bond length slightly. Indirect support for the theoretical prediction of a $^3\Pi_u$ ground state comes from the failure to observe the $^3\Sigma_u^- \leftarrow {}^3\Sigma_g^-$ band system (well known from emission studies) in a jet-cooled beam of aluminum clusters (106). Further support comes from the work of Cai *et al.* (107) who have observed two absorption bands that they have interpreted in terms of a ground state with a vibrational frequency of 284 cm^{-1}: this is in good agreement with the theoretical prediction of 277 cm^{-1} for the $X^3\Pi_u$ state (62) and in clear disagreement with the known frequency (350.0 cm^{-1}) (108) for the $A^3\Sigma_g^-$ state.

C_2, Si_2 and N_2^{2+} are valence isoelectronic, but only for C_2 has there been an experimental determination of the ground state (108). Since these molecules contain multiple bonds, in addition to calibrating the n-particle treatment with the FCI approach, we also performed extensive calculations on C_2 to compare with experiment. Despite the very large correlation energy associated with multiple bonds, the CASSCF/MRCI approach was in excellent agreement with the FCI for the spectroscopic constants. When this approach was applied to C_2 using an extensive ANO basis set, excellent agreement (to within 60 cm^{-1}) was obtained with the experimental separations between the $X^1\Sigma_g^+$, $a^3\Pi_u$ and $b^3\Sigma_g^-$ states (71). Similar theoretical calculations (71) applied to the Si_2 molecule resulted in a determination of the ground state as $X^3\Sigma_g^-$, and the prediction that the $A^3\Pi_u$ state lies 440 ± 100 cm^{-1} higher. The error bars are assigned based on the C_2 calculations, the difference between the MRCI and FCI calculations, and the convergence of the energy separations with expansion of the ANO basis set. Application of the same CASSCF/MRCI treatment to N_2^{2+} (109) yields a $^1\Sigma_g^+$ ground state in analogy with C_2. In fact, the $a^3\Pi_u - X^1\Sigma_g^+$ separation is very similar to that found in C_2, although the $b^3\Sigma_g^-$ state is higher lying in N_2^{2+}. An analysis of both the C_2 and N_2^{2+} wave functions indicates that there is a change in the relative importance of the

major CSFs between the CASSCF and MRCI wave functions. This is one reason that such high levels of correlation treatment are needed for these systems. The FCI calibration calculations were instrumental in showing that the CASSCF/MRCI calculations accurately accounted for the effects of valence correlation on the energy separations. The ability of theory to accurately treat these systems is a major advantage, as spectroscopic determination of the ground states is very difficult.

In addition to the calculation of accurate separations, the calculation of properties is important for an understanding of spectroscopy. We now consider the accurate calculation of the dipole moment function of the $X^2\Pi$ ground state of OH to determine the strength of the rotational-vibrational bands (Meinel system) (110), which are observed in the night sky, in oxygen-supported flames, in the photosphere of the sun, in OH stars, and in interstellar space. Recently, it has been conjectured that the surface-originating glow observed on the Atmosphere Explorer Satellites (111) (and possibly the Space Shuttle) is at least partially due to vibrationally excited OH radicals arising from the collision of the surface with $O(^3P)$ atoms with a relative translational energy of 5 eV.

To determine an accurate electric dipole moment function (EDMF) for the $X^2\Pi$ state of OH requires a very high level of correlation treatment, since it is necessary to properly account for the O^- character in the wave function. To calibrate approximate methods, an FCI dipole moment was computed (61) at five representative r values using a [4*s* 3*p* 2*d*/2*s* 1*p*] Gaussian basis set. Of the variety of approximate methods compared with the FCI, the CASSCF/MRCI treatment reproduced the FCI results best, with an error of only 0.001 a_0 in the position of the dipole moment maximum. The MRCI spectroscopic constants are also in excellent agreement with the FCI. At this level of correlation treatment, it did not make a substantial difference whether the dipole moment was evaluated as an expectation value or as an energy derivative. Having identified an approximate correlation treatment that accurately reproduced the FCI EDMF in a realistic one-particle basis set, this treatment was then carried out in an extended [6*s* 5*p* 4*d* 2*f* 1*g*/4*s* 3*p* 2*d*] ANO basis set. This calculation gave a permanent dipole moment that is within 0.01 D of the experimental value (112) for v=0, and within 10% of the accurate experimental value for the difference in dipole moments between v=0 and v=1. Rotational-vibrational line strengths determined from this theoretical EDMF are expected to be more accurate than those deduced from a variety of experimental sources.

Theory has made a substantial contribution to the determination of accurate electronic transition moment functions (TMF) and radiative lifetimes for atomic and molecular systems. (See, for example, the recent review articles by Werner and Rosmus (113) and Oddershede (114).) However, only recently has it become possible to evaluate unambiguously, using FCI benchmarks, the quality of approximate correlation methods for determining TMFs. The OH ultraviolet system ($A - X$) is important in many applications, such as combustion diagnostics, and is amenable to FCI calculations. Further, there is a large variation in the measured lifetimes, which range (with 1 standard deviation) from 625±25 ns for experiments based on the Hanle effect (115) to 760±20 ns (116) using the high frequency deflection (HFD) technique. The lifetimes measured by laser excitation fluorescence (LEF) range from 686±14 ns (117) and 693±10 ns (118) to 721±5 ns (119).

We have studied (63) the convergence of the $A - X$ TM of OH with respect to convergence of both the one-particle and n-particle spaces. The FCI calibration studies indicated that the state averaged (SA)-CASSCF/MRCI calculations reproduced the FCI value to within 0.2%, but that this required including a δ orbital in the CASSCF active space. Further, a basis set exploration showed that the [6s 5p 4d 2f 1g/4s 3p 2d] ANO basis set employed in our study is probably within 1% of the basis set limit for the transition moment. Thus the computed radiative lifetime of 673 ns for the $A^2\Sigma^+(v'=0,\ N'=1)$ state of OH is expected to be a lower bound and accurate to about 2%. This value is in excellent agreement with two of the LEF values. The theoretical calculations are sufficiently accurate to rule out the somewhat lower value determined by Hanle effect studies, and the higher values determined for the $v'=0$, $N'=1$ level by the HFD technique. The HFD lifetimes for higher N' values, however, are in relatively good agreement with theory — see Fig. 1 where we have plotted the lifetime for $v'=0$ as a function of rotational level. Since the lifetimes are expected to increase monotonically with N' in the regime where the lifetimes are unaffected by predissociation, theory suggests that there may be a systematic error in the HFD lifetimes for small N', perhaps due to collisional quenching.

The OH applications discussed here involve transitions between valence states. The application of the SA-CASSCF/MRCI approach to valence-Rydberg transitions poses additional problems. The requirement of adding diffuse orbitals to the one-particle basis set to describe the Rydberg character is well known, so we fo-

cus on the requirements for the n-particle treatment (68). An excellent system for such a calibration is the AlH molecule, which can be treated very well as a four-electron system, since L-M intershell correlation introduces only a small bond contraction (120,121). The FCI study of AlH included the $X^1\Sigma^+$ and $A^1\Pi$ valence states and the $C^1\Sigma^+$ Rydberg state — see Fig. 2. A relatively small basis set was used, but one that was capable of describing the Rydberg character of the C state. The $A^1\Pi - X^1\Sigma^+$ transition moment is well described by an SA-CASSCF procedure that includes the Al $3s$ and $3p$ and H $1s$ orbitals in the CASSCF active space. As the $C^1\Sigma^+$ state is derived from the $^2S(3s^24s^1)$ state of Al, the active space must be expanded beyond the valence orbitals. When the $4s$ is added to the active space, all MRCI properties except the dipole moment of the C state are in good agreement with the FCI. Since the $C^1\Sigma^+$ state is very diffuse, small changes in the shape of the Rydberg orbital lead to very large changes in the dipole moment. The CASSCF active space must be increased by two σ, two π and one δ orbital in order to compute an accurate dipole moment for the $C^1\Sigma^+$ state. Thus, the SA-CASSCF/MRCI approach is well suited to the study of transitions that involve Rydberg character, with only the minor complication that one or two extra orbitals must be added to the active space. However, if the Rydberg state dipole moment function is required, more substantial augmentation of the active space is needed.

We now turn to the accurate calculation of dissociation energies (D_e), which is a more challenging task than either properties or energy separations between states, because the calculations must be sufficiently flexible to describe the very different molecular and atomic correlation effects equally. Thus only methods that compute a very large fraction of the total valence correlation energy can accurately account for the differential correlation contribution to D_e. We first consider the calculation of D_e for singly-bonded systems.

The dissociation energy of NH is of astrophysical interest for the determination of its abundance in comets and the sun. It is also of interest in modelling the kinetics of rich ammonia flames. However, the experimental determinations since 1970 have ranged from 3.21 to 3.78 eV and even the recommended values are in disagreement (122,123). Quite recently a lower bound of 3.32±0.03 for D_0 was determined using two-photon photolysis of NH_3 (124). The best estimate is obtained by combining this lower bound with an upper bound of 3.47 eV, determined from the predissociation of the $c^1\Pi$ state (125). Thus the D_0 of NH is an order of magnitude

more uncertain than that of CH or OH, which leads to unacceptably large errors in the astrophysical or kinetic modelling. Since CASSCF/MRCI calculations for OH in a large ANO basis set gave a D_e value within 0.03 eV of the accurate experimental value (108), analogous calculations for the $X^3\Sigma^-$ state of NH are expected to yield results of comparable accuracy. Thus an accurate D_e value can be computed for NH by using the FCI approach to calibrate the n-particle treatment and then applying the same level of theory to CH and OH where accurate D_e values are known experimentally. The FCI calibration calculations (60) showed that the CASSCF/MRCI treatment gave equally good D_e values for CH, NH, and OH. The D_0 values for CH, NH and OH, obtained using the CASSCF/MRCI approach in a large ANO basis set, are summarized in Table VI. A comparison of theory and experiment for CH and OH indicates that the calculations underestimate the D_0 values by about 0.03 eV. Since comparable accuracy is expected for all three systems, we can accurately estimate the D_0 value of NH by adding 0.03 eV to the calculated value. The directly computed value cannot be too small, as the ANO basis sets have virtually no superposition error, and it is highly unlikely that the error in NH is twice that of CH or OH, so we are able to assign an uncertainty of 0.03 eV to our recommended value of 3.37 eV. This theoretical prediction is consistent with, but just slightly less than, a very recent experimental determination (126).

The calculation of a D_e for a multiply-bonded system or those with many electrons is even more difficult than for the singly-bonded first-row hydrides such as NH or OH. We have carried out a systematic study (127) of the D_e values of N_2, O_2, and F_2 to evaluate how the errors in the application of the computational methodology vary with the degree of multiple bonding. FCI calibration calculations in a realistic basis set are only possible for N_2 and O_2, and then only with the restriction that the correlation treatment is restricted to the $2p$ electrons. For both the $X^1\Sigma_g^+$ state of N_2 and the $X^3\Sigma_g^-$ state of O_2, the CASSCF/MRCI treatment correlating the $2p$ electrons accounts for essentially all of the correlation effects on the spectroscopic constants — see Table II. For N_2 this treatment in a large ANO basis set produces a D_e value that is larger than experiment (108) (see Table VII). Since this basis set has virtually no CI superposition error, this conclusively shows that $2s$ correlation reduces the D_e value. Subsequent MRCI calculations including $2s$ correlation confirm this conclusion, as the MRCI(10) (that is, ten electrons correlated) D_e value is 0.16 eV less than experiment. The decrease in D_e when the $2s$ electrons are

correlated can be explained in terms of an important atomic correlation effect that has no analog in the molecular system, namely the $2s \rightarrow 3d$ excitation with a recoupling of the $2p$ electrons. The fact that the loss of this atomic effect between infinite separation and r_e could lead to an MRCI(6) value that was too large had been suspected (128), but these calculations dramatically demonstrate the effect. At the MRCI(10) level (based on the CASSCF reference space from the six-electron calculation — CASSCF(6)) the error in D_e is about 4 kcal/mole, or larger than the 1 kcal/mole desired for chemical accuracy. Recent calculations (129) show that part of the error in the MRCI(10) calculation arises from inadequacies in the n-particle treatment: the MRCI reference space must include all possible distributions of the $2s$ and $2p$ electrons in the $2s$ and $2p$ orbitals (note that while the MRCI reference space is expanded, the orbitals are taken from the CASSCF(6) calculation), and part of the error is due to limitations in the one-particle space. Of the remaining one-particle errors, adding more ANOs from the previous primitive set (s through g functions) is the most important factor. Further saturation of the s through g spaces and higher angular momentum functions (h and i type functions) are of about the same importance as the errors in the n-particle space. Ideally one would like to use an FCI calculation to calibrate the errors in the n-particle space, including the N $2s$ electrons. However, this is not possible currently. Nevertheless, the FCI calculations and the systematic improvement of the one-particle basis sets obtained using ANO sets give new insight into the requirements for computing the D_e of N_2.

The results for the D_e value of O_2 are in better agreement with experiment than for N_2; an error of only 1.7 kcal/mole, or only about twice that found for the hydrides. For F_2, FCI calibration calculations are not currently possible, even with $2s$ correlation excluded. However, as in N_2, the insight obtained from other benchmark calculations (29) suggest that to describe the F^-F^+ character in the wave function an "extra" set of π orbitals should be added to the CASSCF active space. With this addition to the active space, the results are significantly improved: even the CASSCF results are now in good agreement with experiment, and the MRCI results in a large basis set yield a D_e with an error of only 0.5 kcal/mole. The agreement is nearly perfect with the addition of the +Q correction. Thus while the electron-dense systems are computationally more difficult, relatively accurate results can still be obtained using MRCI methods. The accuracy is improved with

the inclusion of the +Q estimate for the higher excitations when the number of electrons correlated becomes large. Multiple bonds place tighter demands on both the one- and n-particle treatments, but the calculations are becoming increasingly accurate as the use of larger CI expansions becomes possible.

In the remainder of this section we consider problems where the understanding of the approximations in the one- and n-particle spaces have allowed important chemical problems to be solved. The CN radical is observed in flames, comets and stellar atmospheres. The $A^2\Pi - X^2\Sigma^+$ red system is particularly important as a nitrogen abundance indicator for red giant stars (130). If the oscillator strength of the red system and the ground state dissociation energy of CN are both accurately known, the observed emission intensity in a stellar atmosphere can be converted into elemental abundances. Unfortunately, there is a large variation in the experimental determinations of both quantities. Thus a systematic theoretical study to provide reliable values for these quantities was undertaken (131).

As discussed for N_2, the computation of accurate bond strengths for multiply-bonded systems is a difficult undertaking, requiring both extensive one-particle basis sets and a high level of correlation treatment. However, by performing analogous calculations for the C_2, N_2 and NO molecules where the D_0 values are much better known, the calculated D_0 for CN could be extrapolated by comparing the experimental and theoretical values for these other multiply-bonded molecules. The $s-p$ promotion and hybridization that can occur for C, but not for N or O, could lead to a different requirement in the n-particle treatment. The possibility that $s-p$ hybridization introduces an error into the computed D_e value of CN was excluded by computing the D_e of CN indirectly from the D_e of CN^- using the experimental EA of C (132) and CN (133). As the two routes agree even though the $s-p$ near degeneracy is not present in C^-, this effect does not appear to introduce any perceptible error in the CN D_e value. In this way we were able to arrive at a final D_0 value of 7.65±0.06 eV, where the estimated error bars represent 80% confidence limits. By increasing the error bars to ±0.10 eV, we believe that the theoretical estimate has a 99% probability of encompassing the correct value.

The calibration of the lifetime of the CN red system was done in two ways: the CN violet system, which is well characterized experimentally, was studied, and the transitions in the isoelectronic N_2^+ molecule analogous to the red and violet system in CN were studied (the Meinel (134) and first negative systems (135)). For

the CN violet, the N_2^+ Meinel, and the N_2^+ first negative systems the theoretical radiative lifetimes agree well with experiment (136-138). Therefore, analogous calculations are expected to yield an accurate radiative lifetime of the CN red system as well. Our computed lifetime of 11.2 μs for the v=0 level of the $A^2\Pi$ state is in excellent agreement with a previous theoretical study (139). Nevertheless, it is significantly longer than the value of 8.50±0.45μs, obtained (140) by extrapolation of time decays to zero pressure following photodissociation of C_2N_2. It is difficult to reconcile this difference, but it is conceivable that there are other decay mechanisms such as intersystem crossing between the $X^2\Sigma^+$ and $A^2\Pi$ states that shorten the experimentally observed lifetime. Other indirect experimental measurements of the intensities (141,142), such as measured oscillator strengths, are consistent with theory or suggest an even longer lifetime. Note also that the lifetimes deduced from analysis of the solar spectrum are consistent with theory if the theoretical D_0 value of 7.65 eV is used in the analysis. Thus the theoretical lifetimes and D_0 value are consistent with the solar spectrum model of Sneden and Lambert (130).

The analysis of cometary data requires knowing the vibrational transition band strengths in the $X^2\Sigma^+$ state of CN. Two very different values for the Einstein coefficient (A) of the fundamental 1-0 vibrational band have been reported: one based on analysis of cometary data (143) and the other from measurements in a King furnace (144). Using the CASSCF/MRCI dipole moment function, the computed A_{10} value (145) was in excellent agreement with the value measured in the King furnace. The small uncertainty in the computed value suggests that some of the assumptions in the model used to analyze the cometary data are in error.

One of the most important chemiluminescent phenomena is the so-called Lewis-Rayleigh afterglow that occurs from the recombination of ground state nitrogen atoms (146). Since most of the emission occurs in the first positive bands (1+) of N_2, which cannot be directly populated in the recombination of ground state atoms, a precursor state must be involved. Berkowitz, Chupka, and Kistiakowsky (BCK) (147) have proposed the $A'\ ^5\Sigma_g^+$ state as the precursor, whereas Campbell and Thrush (148) invoke instead the $A^3\Sigma_u^+$ state. The main objection to the BCK theory was that the binding energy of the $A'\ ^5\Sigma_g^+$ state (estimated (149) at the time to be ≈850 cm^{-1}) was not sufficient to maintain an appreciable steady-state population.

Recent theoretical calculations (150) on the $A'\ ^5\Sigma_g^+$ state potential again il-

lustrate that accurate results for the binding energy require both extensive treatments of electron correlation and a large one-particle basis set. On the basis of CASSCF/MRCI calculations using a large ANO basis set, the $A'\ ^5\Sigma_g^+$ potential was found to have an inner well with a depth of about 3450 cm^{-1} and a substantial barrier ($\approx$500 cm^{-1}) to dissociation. Figure 3 shows the $B^3\Pi_g$, $A^3\Sigma_u^+$ and $A'^5\Sigma_g^+$ potential curves and their vibrational levels in the region of interest. The explanation for most of the experimental observations is apparent from these potentials. For example, the barrier in the $A'^5\Sigma_g^+$ state yields a quasibound level that allows intersystem crossing from the A' state to v'=13 of the $B^3\Pi_g$ state. The observation that $v' = 13$ is populated by the same mechanism as $v' \leq 12$, and that emission from $v' \leq 13$ is similar, but markedly different from $v' > 13$, even though $v' = 13$ is above the energy of the separated atoms, is consistent with the barrier in the theoretical potential. At 300 K the maximum intensity originates from v'=11 in the $B^3\Pi_g$ state. This arises since the A' state is vibrationally relaxed before intersystem crossing to the B state, i.e. the lowest vibrational level of the A' state most efficiently crosses to $v' = 11$ in the B state. At 77 K, an outer van der Waals well in the A' state (not shown in the figure), allows for tunnelling to the higher vibrational levels of the inner well of the A' state. Since there are fewer collisions at this reduced temperature, intersystem crossing to the $v' = 12$ level of the $B^3\Pi_g$ state is more rapid than collisional relaxation, causing the maximum intensity in the $B^3\Pi_g$ state emission to increase from $v' = 11$ to $v' = 12$. At 4 K the barrier in the A' state leads to a cutoff in the emission from $v' = 10 - 12$. However, the $A^3\Sigma_u^+$ state has no barrier and therefore it populates the $B^3\Pi_g$ state even at 4 K. We note that the $A^3\Sigma_u^+$ and $B^3\Pi_g$ potential curves cross at $v = 16$ in the A state and v'=6 in the B state, thereby giving a maximum in emission for the v'=6 level of the B state at 4 K. Therefore, the calculations indicate that the $A^3\Sigma_u^+$ and $A'^5\Sigma_g^+$ states are both important precursors in populating the B state. The deep well in the $A'^5\Sigma_g^+$ state, revealed for the first time by these calculations, eliminates most of the objections to the original BCK theory.

Part of the emission in the Lewis-Rayleigh afterglow involves the Hermann infrared system (HIR). This band system consists of a group of unclassified multiheaded bands in the region 700-970 nm. Although the system was unassigned, it was known [151] that the bands were produced by either a triplet or quintet transition and that the system was readily generated from the energy pooling reaction

between metastable $N_2(A^3\Sigma_u^+)$ molecules. As part of our theoretical study (150) of the N_2 afterglow, we found that the HIR band positions and intensities corresponded exceptionally well to our theoretical values for the $C''^5\Pi_u - A'\ ^5\Sigma_g^+$ transition– see Table VIII. This, combined with the fact that the energetics are consistent with an energy pooling reaction preferentially populating the v'=3 level of the $C''^5\Pi_u$ state (152), provided rather convincing evidence for the assignment of the HIR system to this transition. This assignment has now been confirmed (153) by a rotational analysis of the $C''^5\Pi_u - A'\ ^5\Sigma_g^+$ band system produced in emission in a supersonic jet discharge.

VIII. TRANSITION METAL SYSTEMS.

The accuracy of calculations on transition metal systems has lagged behind that of the first and second rows of the periodic table (154). One problem for the transition metal compounds is that an SCF wave function is often a much poorer representation of the system than for those compounds only composed of first- and second-row elements. In fact, for some transition metal systems large CASSCF calculations are required even for a qualitatively correct description, and a quantitative description requires lengthy CI expansions. In addition to extensive n-particle basis requirements, experience has shown that transition metals also require considerably larger one-particle basis sets than for the first and second rows. As transition metals have such stringent one- and n-particle requirements, FCI benchmark calculations and ANO basis sets have given considerable insight into how to improve the accuracy of calculations on transition metal systems.

A common feature of transition metal calculations is that several atomic asymptotes are involved in the bonding: this mixing is much more prevalent for transition metal systems than non-transition metal systems and much harder to describe accurately. For example, in the transition metal hydrides it has been shown that the $d^n s^2$, $d^{n+1}s^1$ and d^{n+2} asymptotes all contribute to the bonding in the low-lying states. The importance of these asymptotes depends on the atomic separations. Further, the magnitude of the $d-d$ exchange energy and the relative size of the s and d orbitals are both important in determining the bonding in the molecular system.

As a first example of calculations on transition metals, we consider the $^5D(3d^6 4s^2) - {}^5F(3d^7 4s^1)$ separation in the Fe atom. FCI benchmark calcula-

tions (58) of this separation, in a basis set that includes an f function, show that for Fe the single-reference SDCI procedure accounts for most of the differential correlation energy in the $3d$ and $4s$ shells. When this SDCI procedure is carried out in a [$7s$ $6p$ $4d$ $4f$ $2g$] basis set and the dominant relativistic effects accounted for, the separation is 1.25 eV: this is significantly larger than the experimental separation (155) of 0.875 eV. Adding the $3s$ and $3p$ electrons to the SDCI treatment reduces the separation to 1.06 eV. It is highly likely that most of the error in the 16-electron calculation comes from errors in the n-particle treatment. However, approximate methods of accounting for higher excitations cannot be reliably used for this problem; the eight electron FCI benchmark calculations showed that the +Q correction and the CPF method incorrectly estimate the differential effect of the higher excitations. This is due to the different character of $4s$ and $3d$ correlation energy contributions: for example c_0 is reduced much more by $4s-4s$ correlation than an equivalent amount of $3d-3d$ correlation. Thus when two states are compared, the +Q correction is reliable only if the state with the larger correlation energy also has the smaller c_0 value. The +Q correction may therefore fail to give reliable results for transition metal systems when different types of correlation effects are included, even though the correction works well in first-row systems when eight or so electrons are correlated. This indicates that caution must be used when applying approximate treatments that account for higher excitations to single-reference-based transition metal calculations. Finally, to compute accurate atomic separations in Fe, and presumably for the metal atoms left of it in the first transition row, it will be necessary correlate the $3s$ and $3p$ electrons.

As noted above the bonding in transition metal systems frequently involves a mixture of several atomic asymptotes. A study (65) of TiH has shown that a CASSCF/MRCI treatment agrees well with the FCI for the spectroscopic constants, but is much poorer for one-electron properties such as the dipole moment. This difference arises because the bonding in the $X^4\Phi$ state of TiH involves a mixture of the Ti $3d^24s^2$ and $3d^34s^1$ atomic occupations. The $3d^34s^1$ occupation forms a Ti $4s$-H $1s$ bond that is polarized toward the H, thus yielding a large dipole moment of Ti^+H^- polarity, while in the $3d^24s^2$ occupation, $4s-4p$ hybridization occurs, with one hybrid orbital polarized toward the H, and the second polarized away from the H. The movement of charge toward the hydrogen is balanced by the movement away, thus the dipole moment associated with the $3d^24s^2$ asymptote is quite small.

Since both asymptotes form strong bonds to the hydrogen, but have very different dipole moments, the energetics are less sensitive to the mixing than the total dipole moment. The FCI studies show that the CASSCF/MRCI method may not yield a reliable dipole moment, since the CASSCF generally includes only the nondynamical correlation and the MRCI is not able to fully account for the orbital relaxation associated with dynamical correlation. However, the benchmark calculations show that the MRCI properties converge to the FCI result if natural orbital iterations are performed, which we denote NO-MRCI. This is different from first-row systems where NO iterations were not required; for example, the CASSCF/MRCI properties for OH are in excellent agreement with the FCI without NO iterations. Therefore, in the study of transition metals at least one NO iteration should be performed to test the convergence of properties.

Since the calculations on TiH showed that the NO-MRCI properties were in good agreement with the FCI, it is expected that this level of treatment in a large one-particle basis should yield very accurate results. NiH is one of the few transition metal systems where the dipole moment (2.4±0.1 D) has been measured (156). At the SCF level, the dipole moment of NiH is much too large (about 4 D), because the wave function is biased strongly in favor of the $3d^9 4s^1$ asymptote of Ni (157). This bias is not fully overcome with low levels of correlation treatment, and at the SDCI level the dipole moment (3.64 D) remains much too large. A CASSCF treatment allows the Ni $3d^8 4s^2$ and $3d^9 4s^1$ asymptotes to mix, but because the $3d^8 4s^2$ state lies over one eV too low at this level, the CASSCF mixes too much $3d^8 4s^2$ character into the wave function resulting in a dipole moment that is too small (1.74 D). Inclusion of more extensive correlation in the MRCI approach gives a better balance between $3d^8 4s^2$ and $3d^9 4s^1$ and a dipole moment (2.15 D) that is closer to experiment. However, the converged NO-MRCI dipole moment of 2.59 D is slightly larger than experiment.

The accurate treatment of weakly bound systems is very difficult, since correlation is required to describe the dispersion, but superposition errors (SE) can be significant at high levels of correlation treatment (82,158). To eliminate the SE, very large primitive sets including many sets of polarization functions are required. Until recently large valence primitive sets were unavailable for the transition metal atoms, making it uncertain whether it was worth studying weakly bound transition metal complexes. Partridge (159) has recently optimized large primitive basis sets

for the first transition row atoms. When these (20s 12p 9d) basis sets are supplemented with a diffuse d function to describe the $3d^{n+1}4s^1$ occupation and three p functions to describe the 4p orbital, they are of the same quality as the (13s 8p) sets for first-row atoms. These large basis sets have a triple-zeta 4s function, and when flexibly contracted and supplemented with extensive polarization sets they yield very small superposition errors. Using the ANO procedure these basis sets can be contracted to a manageable size. As an example we consider the Ni-H_2O system (85). This study used a (20s 15p 10d 6f)/[7s 6p 4d 3f] contraction for Ni, a (14s 9p 6d 4f)/[6s 5p 4d 2f] contraction for O, and an (8s 6p)/[4s 3p] contraction for H. At the SDCI level, the total superposition error is only 0.53 kcal/mole or about 10% of the binding energy. The Ni superposition error was only about twice that of the water. As discussed in Ref. 85, previous studies of the binding energy had obtained spuriously large values as a result of superposition error. Thus with the current large primitive basis sets and improved contraction schemes it is now possible to study weakly-bound transition metal systems.

As a further example of accurate calculations for a transition metal system, consider the difficulty of determining the ground state of FeH. The laser photodetachment spectroscopic studies of FeH^- by Stevens *et al.* (160) have been interpreted in terms of a $^4\Delta$ ground state and a low-lying $^6\Delta$ state only 0.25 eV higher. However, the $^4\Delta - {}^4\Delta$ infrared system, which has been observed in the absorption spectra of heated mixtures of iron metal and hydrogen, has not yet been observed at low temperatures in matrix studies (161). Although early theoretical calculations (162) placed the $^6\Delta$ state lower, qualitative arguments, based on the r_e values of the $^4\Delta$ and $^6\Delta$ states of FeH and the $^5\Delta$ ground state of FeH^- in relation to the width of the peaks in the photodetachment spectra, supported the interpretation of a $^4\Delta$ ground state by Stevens *et al.* (160). However, more accurate calculations are now possible using ANO basis sets and large-scale MRCI calculations (163). For example, a CASSCF/MRCI+Q calculation, correlating the eight valence electrons in a large [8s 7p 5d 3f 2g/4s 3p 2d] ANO Gaussian basis set, predicts the $^4\Delta$ state to be 0.06 eV lower than the $^6\Delta$ state. (Note that the +Q correction should be qualitatively correct since the differential contribution from c_0^2 and the correlation energy work in the same direction). The $^4\Delta - {}^6\Delta$ separation is further increased to 0.16 eV when a correction for 3s and 3p inner-shell correlation is included based on MCPF calculations. Most of the remaining discrepancy with the experimental

estimate of 0.25 eV for the separation is probably due to underestimating the differential effects of inner-shell correlation. Therefore, these theoretical predictions provide strong support for the interpretation of the photodetachment spectra of Stevens *et al.* (160) in which the $^6\Delta$ state is placed above the $^4\Delta$ ground state. Nevertheless, FeH represents a very difficult case for theory, namely the presence of two nearly degenerate states of different multiplicity. Very high levels of correlation treatment are required to quantitatively account for the separation as the correlation energy is substantially larger for the lower spin state. The failure to observe the $^4\Delta - {}^4\Delta$ infrared system in absorption at low temperature is probably due to the broadening of this already weak band system by the matrix (160).

The difficulty in computing an accurate $^4\Delta - {}^6\Delta$ separation in FeH arises mostly from the large $3d-3d$ exchange energy resulting from the compact nature of the $3d$ orbital. Although the large loss in exchange energy from reversing the electron spin is balanced by the greater bonding in the $^4\Delta$ state of FeH, this latter effect requires high levels of correlation treatment to describe. Thus low levels of correlation treatment favor the $^6\Delta$ state, resulting in the incorrect ordering of states. This situation can be contrasted with the $^1A_1 - {}^3B_1$ separation in CH_2. More accurate results are possible in the latter case, because the differential exchange and bonding contributions are much smaller.

IX. THE CALCULATION OF POTENTIAL ENERGY SURFACES

In the previous sections we have discussed the application of the most accurate theoretical methods for the calculation of spectroscopic constants. Another important area of computational chemistry is dynamics (164). A variety of methods have been developed for the determination of scattering cross sections, rate constants and product state distributions. These dynamical methods, either classical or quantum mechanical, require knowing the form of the potential energy surface (PES). Therefore, the accuracy of the predictions of these dynamical methods ultimately depends on the accuracy of the PES. It is clear that single-reference-based methods will not be able to describe the bond breaking and bond formation that occur during a reaction. They may, however, yield accurate surfaces for non-reactive collisions. The multireference-based approaches appear to be the only alternative for the accurate calculation of general PESs. Given the kind of insight that the FCI calibration has given into the n-particle approximations for spectroscopic problems and the high

accuracy that the ANO basis sets have shown for these classes of problems, it is important to test these advances on the calculation of PESs. Unfortunately it is not possible to directly compare a theoretical PES with experimental observations, and therefore some of our conclusions will have to wait for confirmation by application of dynamical studies to our PESs.

The first system we consider is the isotope exchange reaction for H_2 and D_2. Experimental studies of this reaction are very difficult to perform since impurities allow the formation of H atoms, which then results in a radical exchange reaction (165). The early theoretical studies were flawed by the assumption that the reaction proceeded by a four-center symmetry-forbidden process (166). While the later theoretical studies (167) focused on the symmetry-allowed termolecular process,

$$2H_2 + D_2 \rightarrow 2HD + H_2 \tag{17}$$

they suffered from limitations in both the one- and n-particle basis sets and contained an uncertainty of perhaps 10 kcal/mole in the barrier height. However, recent calculations (70) have reduced this uncertainty to less than 1 kcal/mole. In that study all calculations were performed on six-electron systems in order to minimize size-consistency errors in the comparisons, so the H_2 results to be quoted were obtained from calculations on three separated H_2 molecules. An FCI treatment in a DZP basis set shows that the CASSCF/MRCI D_e of H_2 is only 0.1 kcal/mole smaller than the FCI, while applying the +Q correction to the six-electron calculation results in a D_e value for each H_2 that is 0.1 kcal/mole too large. There is essentially no difference in the saddle-point geometry between the FCI, MRCI, or MRCI+Q calculations, and the barrier heights are also in good mutual agreement: 70.9(MRCI), 70.4(MRCI+Q) and 70.4(FCI). The MRCI calculations were then repeated in an ANO basis set that yields a D_e value for H_2 at the MRCI+Q level (for a system of three separated H_2 molecules) that is only 0.3 kcal/mole smaller than experiment. The barrier height at the MRCI and MRCI+Q levels is 66.5 and 67.4 kcal/mole, respectively. Based on the FCI calibration in the DZP basis set, we expect that the true barrier height lies between these values. As the error in the barrier height should be smaller than the error for the process of dissociating the three H_2 molecules to six H atoms, the barrier should be accurate to better than 1 kcal/mole, which is comparable to or better than experiment.

The F+H_2 →FH+H reaction has received considerable attention from the-

ory (168-174) as it is an excellent system for the calibration of methods: there is experimental data for the reaction rate as a function of temperature, information on product vibrational energy distribution, and the reaction thresholds are known for both H_2 and D_2 (175,176). In Table IX, several different treatments are compared to the FCI barrier height and exothermicity (55,168,169); in all of these treatments only seven electrons (F $2p$ and H $1s$) are correlated. The smallest MRCI treatment has the F $2p\sigma$ and H $1s$ orbitals active in the CASSCF and MRCI (denoted MRCI(300), since there are three active orbitals of a_1 symmetry). This calculation yields a barrier height that is 0.68 kcal/mole higher than the FCI value. The inclusion of the +Q correction improves the barrier height, but it is now slightly too small. The sign of the error in the exothermicity also changes with the addition of the +Q correction. Such problems with the MRCI(300) treatment are not unexpected since the HF wave function is known to contain significant H^+F^- character. For accurate results it is therefore necessary to improve the description of the electron affinity (EA) of F by expanding the active space to include $2p_\pi \rightarrow 2p'_\pi$ correlation. With such a (322) active space, a very large number of CSFs would arise in a CASSCF reference MRCI wave function, so it becomes necessary to select reference CSFs according to their CASSCF coefficients as described in Section II: with this expanded active space the MRCI(322)+Q results are in excellent agreement with the FCI, provided that the threshold for including CASSCF CSFs as references is no larger than 0.025. Further expansion of the active space improves the results, but the +Q correction is now too large. The ACPF method was also used to estimate the effect of higher excitations. The ACPF results are better than MRCI(322)(0.025), but not as good as MRCI(322)(0.025)+Q. The differences are relatively small, however. It was also found in an ACPF treatment in a large basis set that a CSF with a coefficient of less than 0.025 in the CASSCF wave function appeared with a much larger coefficient in the ACPF wave function near the saddle point. This configuration corresponds to an ionic $F^-H_2^+$ contribution, and its inclusion (making 13 reference occupations) has little effect in the small basis set that does not adequately describe F^-. However, it has an important effect in the larger basis set, where F^- is described much better. In addition, we note that singles, doubles, triples and quadruples away from an SCF reference (SDTQCI) has a comparable error to the ACPF, but of opposite sign.

As we noted in the beginning of this section, single-reference-based techniques

are not expected to be quantitative, but they can still be very useful in preliminary calculations. In this regard we note that although the CPF method is quite accurate for the barrier height and saddle-point geometry, it is significantly poorer than the MRCI for the exothermicity.

In order to compute an accurate barrier height, the basis set is expanded from the [4*s* 3*p* 1*d*/2*s* 1*p*] set used for the FCI calibration to a [5*s* 5*p* 3*d* 2*f* 1*g*/4*s* 3*p* 2*d*] ANO set. In this large basis set, the spectroscopic constants for H_2 are in almost perfect agreement with experiment. The MRCI(222)+Q treatment of HF, which is analogous to the MRCI(322) treatment of F+H_2, yields an excellent r_e, but a D_e value that is 1.22 kcal/mole (0.05 eV) too small. The CI superposition error for F is 0.15 kcal/mole; this is even smaller than that obtained using the large Slater-type basis se[illegible]om Ref. 170. An analysis of the wave function shows that the saddle point resembles F+H_2 more than HF+H. Therefore, the barrier height should be accurate to better than 1 kcal/mole.

The theoretical results for the classical saddle-point and barrier height are summarized in Table X. Based on the FCI calibration calculations, the MRCI(322)(2*p*)+Q calculations with seven electrons correlated (i.e. excluding F 2*s* correlation), are expected to reproduce the result of an FCI calculation in a nearly complete one-particle basis set. Since F 2*s* correlation decreases the barrier, this MRCI(322)(2*p*)+Q barrier, when corrected for the CI superposition error (SE), represents an absolute upper bound of 2.52 kcal/mole for the barrier height. The ACPF(322)(2*p*) barrier height is slightly higher than the MRCI(322)(2*p*)+Q barrier height as expected from the FCI calibration calculations. This illustrates that the one and *n*-particle basis sets are not strongly coupled, as both methods of estimating the higher excitations agree in two different basis sets.

The inclusion of F 2*s* correlation decreases the barrier height, and increases the magnitude of the +Q correction. Unlike the seven-electron treatment, the ACPF(322) and MRCI(322)+Q results do not agree as well when nine electrons are correlated. Unfortunately, it is not possible to calibrate this level of treatment using the FCI approach in a realistic one-particle basis set. However, the ACPF wave function shows that there is an $F^-H_2^+$ contribution to the wave function that is not accounted for by simply adding the extra π orbitals to the active space. As noted previously, it is necessary to add an additional CSF to the reference list to bring the MRCI and ACPF barrier heights into agreement. The additional CSF significantly

changes the ACPF barrier, but does not affect the MRCI barrier and increases the MRCI+Q barrier only slightly. The agreement of the two methods gives strong support for a conservative estimate of 2.00 kcal/mole for the barrier height, after correction for SE. A more realistic value for the barrier height should account for basis set incompleteness and the underestimation of the effects of higher excitations by the +Q correction: we assume that the +Q estimate is too small, since the difference between the size-consistent ACPF(322)(2p) and ACPF(322) treatments is larger than the difference between the MRCI(322)(2p)+Q and MRCI(322)+Q treatments. Our best empirical estimate of 1.60 kcal/mole is obtained by omitting the SE correction, adding instead 0.1 kcal/mole for basis set incompleteness and a further correction of 0.1 kcal/mole for an understimation of the +Q reduction to the classical barrier height. Thus based solely on estimates from *ab initio* calculation, the barrier height should be between 1.60 and 2.00 kcal/mole.

Our estimate is very similar to that made by Truhlar and co-workers (171) using the scaled external correlation (SEC) method, but different from that suggested by Schaefer (174) (i.e. a barrier height greater than 2.35 kcal/mole) or the Monte Carlo calculations (172) that yield a barrier of 4.5±0.6 kcal/mole. The lower bound for the barrier suggested by Schaefer (174) appears to be supported by SDTQCI results (173) (correlating only 7 electrons), that yield a barrier of 2.88 kcal/mole. Further, no differential effect of F 2s correlation is observed at the SDTQCI level in a small basis set. However, the basis sets used in the SDTQCI calculations are far from the one-particle limit. If an estimate for errors in the one-particle basis is included, the SDTQCI results are found to be in good agreement with the MRCI(322)(2p)+Q and ACPF(322)(2p) methods, as expected based on the FCI calibrations. Therefore, the only difference between the MRCI (or ACPF) and SDTQCI is the effect of F 2s correlation on the barrier. In Table XI we give the results of FCI benchmark calculations correlating nine electrons in a DZ+p_F (double-zeta plus diffuse p on fluorine) basis. As we discussed above, for realistic benchmarking a larger basis set is required. This is clear from the fact that at the seven-electron level in the larger basis set the barrier height is MRCI>ACPF>MRCI+Q>FCI>SDTQCI, while in the smaller basis set it is SDTQCI>MRCI>FCI>ACPF>MRCI+Q. These calculations are only qualitative, but they do suggest that the SDTQCI calculation underestimates the differential effect of the F 2s correlation. Thus, even a single-reference-based technique that correctly includes both triple and quadruple

excitations is inferior to the CASSCF/MRCI approach. We also feel that the deficiencies of the Monte Carlo method are related to the use of a single reference to fix the nodes: the *ab initio* results clearly show that the wave function near the saddle point has a much greater multireference character than the wave function for either the products or reactants.

While the MRCI(322)+Q (or ACPF(322)) calculations in the ANO basis set are more reliable than any previous results, considerable computer time would be required to compute a global surface at this level. The barrier height was therefore investigated using the contracted CI (CCI) approach. In the same large ANO basis set, the CCI+Q barrier is 0.4 kcal/mole higher than the corresponding MRCI+Q value. Modification of the basis set was also investigated at the CCI level: f polarization functions on H were found to lower the barrier by only 0.07 kcal/mole, while eliminating the g function on F increased the barrier by 0.12 kcal/mole. These observations are consistent with the contention that the basis set is effectively complete. The CCI calculation in this basis set is sufficiently inexpensive that much larger regions of the PES can be investigated. Of course, given the difference between the MRCI and CCI barrier heights, some account would have to be taken of the errors in CCI treatment; this might involve adjusting the parameters in the fitted potential based on the MRCI(322)+Q calculation or on information deduced from experiment.

While the CCI+Q PES scaled using the MRCI(322)+Q results should be accurate, direct comparison with experiment is difficult. To facilitate comparison we have employed canonical variational transition state theory (177) at the classical and adiabatic barrier using the CCI+Q potential for both $F+H_2$ and $F+D_2$. These calculations account for the zero-point energy and include a tunnelling correction. The results of these calculations are summarized in Table XII. As expected, the zero-point and tunnelling corrections are different for H_2 and D_2. At the classical saddle point, the barrier heights for H_2 and D_2 differ by 0.2 kcal/mole, whereas at the adiabatic saddle point the barriers are essentially the same. The observation (175,176) of nearly identical thresholds for H_2 and D_2 also provides strong support for using the adiabatic barrier. In order to bring the computed threshold into agreement with experiment (175,176), we must lower the CCI+Q classical barrier by 0.7−0.8 kcal/mole. This produces a barrier height of 1.3−1.4 kcal/mole, or after accounting for the errors associated with various approximations, a barrier

height of 1.0−1.5 kcal/mole. This is in good agreement with the estimate made directly from the various multireference treatments, and also with that deduced in recent calculations by Truhlar and co-workers (171), although it disagrees with the value inferred by Schaefer (174) from most previous calculations.

The previous two applications consider dynamical problems where only the ground state potential energy curve is of interest. However, this is not always the case — many situations involve a curve crossing. While most scattering formalisms are developed in a diabatic representation, a theoretical PES is computed in the adiabatic representation. Hence when curve crossings (or more complicated phenomena for polyatomic systems) occur both potentials must be accurately represented in the crossing region, and nonadiabatic coupling matrix elements (NACMEs) will be required to define the unitary transformation between the diabatic and adiabatic representations. Until recently, NACMEs were computed either using finite difference methods (178) or via approximations to avoid computing matrix elements between nonorthogonal wave functions (179,180). However, Lengsfield, Saxe, and Yarkony (181,182) have recently developed an efficient method of evaluating NACMEs based on state-averaged MCSCF wave functions and analytic derivative methods. This should provide NACMEs of similar overall accuracy to that obtained for the adiabatic potentials.

To accurately describe curve crossings requires, in addition to the NACMEs, an equivalent treatment of both states involved in the crossing. In curve crossings where the molecular orbitals for the two states are similar, such as interactions between valence states derived from diff nt asymptotic limits, the CASSCF/MRCI approach would be expected to describe both potentials accurately irrespective of which state is used for the orbital optimization. However, when the character of the two states is very different, such as valence/Rydberg mixing (68) or interaction between states derived from ionic and covalent limits (69), it is more difficult to achieve equivalent accuracy for the lowest adiabatic state on either side of the crossing point. This is commonly the case for charge-exchange reactions, such as $N^+ + N_2 \rightarrow N + N_2^+$, or chemi-ionization processes such as $M + X \rightarrow M^+ + X^-$, where the optimal molecular orbitals for the ionic and neutral solutions differ greatly. To gain additional insight into the computational requirements for describing the potentials in the region of curve crossings, we have studied (69) the $Li + F \rightarrow Li^+ + F^-$ chemi-ionization process using the FCI approach. In LiF, the lowest adiabatic state

at short r values, namely the ionic $X^1\Sigma^+$ state, dissociates adiabatically to neutral ground-state atoms. There is an avoided crossing at the point where the energy difference between the F electron affinity (EA) and the Li ionization potential exactly balances the $1/r$ electrostatic stabilization. Since the CASSCF description of F^- is poor (29), the CASSCF estimate for the bond distance at the crossing point is unrealistically small. When orbitals from the ground-state CASSCF wave function are used to construct an MRCI wave function, the CASSCF description of the crossing point will compromise the accuracy of the MRCI description. This problem is not easily resolved by expanding the CASSCF active space, as very large active spaces are required to obtain a good description of the atomic electron affinities. However, by performing instead an SA-CASSCF calculation, in which the orbitals are optimized for the average of the two lowest $^1\Sigma^+$ states in LiF (the ionic and neutral states), the orbital bias is eliminated and the MRCI treatment is in excellent agreement with the FCI. It is also important to note that this averaging does not significantly degrade the description of the system near r_e. Thus state averaging appears to be an excellent method of achieving equal accuracy for two potential curves in a curve crossing region, and should also perform well for polyatomic systems. The utility of state averaging as a means of obtaining a good compromise set of orthogonal molecular orbitals for use in an MRCI wave function has also been found to be an excellent route to computing accurate electronic transition moments (63), as noted above. Thus there is much in common between methods that account accurately for differential correlation effects on a PES and those that yield accurate spectroscopic constants and molecular properties.

Application of the SA-CASSCF/MRCI approach to the LiF curve crossing in a $(13s\ 9p\ 6d\ 4f)/[4s\ 3p\ 2d\ 1f]$ F and $(14s\ 7p\ 4d)/[5s\ 4p\ 2d]$ Li basis set yields smooth dipole moment and potential energy curves, as expected. These calculations were able to demonstrate that the previous failure of an analysis of the curve crossing was due to poor adiabatic potentials, not the use of the qualitative Rittner model (180). The NACMEs deduced from the SA-CASSCF/MRCI calculation are in good agreement with other determinations (183). The limitations in these calculations arise from the difficulty in computing the EA of F. As we discuss in the next section, this is still a very challenging task. As our ability to compute electron affinities improves, the accuracy of such ionic-covalent curve crossings will also improve, as the FCI benchmarks have shown that the SA-CASSCF/MRCI calculations are correctly

describing this region of the potential.

The applications considered in this section illustrate that current methods are yielding more accurate potential energy surfaces, although it is often too expensive to compute entire PESs using very extensive MRCI calculations. However, with advances in surface fitting techniques it may be possible to merge accurate calibration calculations at critical points on the PES with global calculations using less computationally expensive methods. For example, we have used the CCI method in a smaller basis set to map out the F + H_2 potential (168). This more approximate level of treatment agrees with the best calculations to within about 1 kcal/mole and is therefore expected to be semi-quantitatively correct. Scaling of these results can thus be expected to yield accurate global surfaces.

X. SYSTEMS WITH A STRONG COUPLING OF THE ONE- AND n-PARTICLE SPACES

In the previous sections we have illustrated how the accuracy of *ab initio* calculations has been greatly enhanced by recent developments. However, there are a few systems where even these new advances have not fully answered the question as to which is the appropriate quantum chemical treatment. These problems involve correlation of core electrons and computation of electron affinities and we first consider core correlation.

As noted above, a high level of correlation treatment is required to fully account for the effect of $3s$ and $3p$ correlation on the $^5D - {}^5F$ separation in Fe atom (58). It is impossible to study inner-shell correlation effects for transition metal systems using FCI benchmark calculations, and furthermore errors associated with other approximations are generally as large. However, the calculations for the $^1A_1 - {}^3B_1$ separation in CH_2 (88) indicate that the treatment of the valence correlation is nearly exact and one of the largest remaining errors is the neglect of correlating the C $1s$ electrons. In addition, as correlating the core in C adds only two extra electrons it is amenable to FCI benchmark calculations. Thus we have investigated (66) the effect of core correlation on the $^1A_1 - {}^3B_1$ separation in CH_2, as well as the C $^3P - {}^5S$ separation. Correlating the core not only places more stringent requirements on the n-particle treatment, it also increases the demands on the one-particle basis set.

The study of the error associated with the ANO contraction procedure on the $^3P - {}^5S$ separation in the C atom shows that while the ANO procedure works

very well for valence correlation, the convergence of the basis set with contraction level for the core-core (CC) and core-valence (CV) correlation is very slow. This is related to the fact that the change in c_0 for a given correlation energy lowering, and hence the size of the natural orbital occupation numbers associated with the core correlation, is smaller than those associated with valence correlation energy. Thus, when both core and valence correlation are included, it becomes impossible to order the NOs based on their contribution to the correlation energy using the occupation numbers, and therefore it is difficult to use the ANO procedure effectively. This is analogous to the origin of the failure of the +Q correction in describing higher excitations in Fe atom. The contraction problem is reduced somewhat when the nearly constant CC correlation is deleted and only the CV correlation is included, but the convergence with contraction level is still much slower than when only valence correlation is included. Note that elimination of the CC correlation also reduces the requirements on the primitive basis set.

In addition to problems associated with the one-particle basis set, the FCI benchmarks show that very high levels of correlation treatment are required to correctly balance the CV (or CC) and valence correlation. This usually involves increasing the active space such that a larger fraction of the valence correlation energy is included in the zeroth-order wave function. In fact, for an MRCI calculation to account for all of the CV effect, the zeroth-order wave function has to account for essentially all of the valence correlation. This leads to a large expansion in the valence part of the problem, which when coupled with the larger basis set requirements and additional electrons being correlated, leads to a much larger computational problem than the study of valence correlation only. Failing to expand the valence treatment adequately can lead to an overestimation of the differential CV contribution even though the total CV correlation energy may be underestimated.

The effect of CV correlation on the $^1A_1 - {}^3B_1$ separation in CH_2 was estimated by using a totally uncontracted C s and p basis set to avoid the contraction problem. Using the C $^3P - {}^5S$ separation as a calibration, it is likely that the largest possible valence active space that could be used in the CH_2 calculations would lead to a slight overestimation of the CV effect. However, even this calculation resulted in a CI expansion of about 1.5 million CSFs. The benchmark studies (66) of CV correlation indicate that it increases the $^1A_1 - {}^3B_1$ separation in CH_2 by about 0.35 kcal/mole — see Table V. Unfortunately, such CV calculations are too large

to be routinely carried out for more complex systems. Thus there is considerable motivation for developing less expensive ways of including this effect, such as the CV operator approach being developed by Meyer and co-workers (184).

The nuclear hyperfine interaction, which depends on the spin density at the nucleus, is very sensitive to CC and CV correlation. To determine even qualitatively correct results for the nitrogen atom hyperfine coupling constant requires correlating the $1s$ orbital (185). Very high levels of correlation treatment as well as large flexibly contracted basis sets are required for quantitative results. Further there is a strong coupling of the one- and n-particle basis sets, which makes it difficult to perform definitive FCI calibration calculations (67). To achieve quantitative agreement between the MRCI and FCI hyperfine constants for N atom, it was necessary to include the $2s$, $2p$, $3s$, $3p$ and $3d$ orbitals in the CASSCF active space. This is consistent with the calculations to determine the C $^3P - {}^5S$ separation, which showed that the zeroth-order reference must account for almost all of the valence correlation energy in order for the MRCI to accurately account for CV and CC effects. Also, the basis set must include several f functions to be within 5% of experiment. In spite of the strong coupling between the basis set and correlation treatment, the FCI calculations demonstrated that diffuse s functions contribute significantly to the spin density, because of an important class of configurations involving $2s \rightarrow 3s$ promotion with a spin recoupling. Thus, the study of the isotropic hyperfine constant of N atom indicates that quantitative agreement with experiment requires very large one-particle basis sets (flexibly contracted in the core and augmented with diffuse and polarization functions), as well as an extensive treatment of electron correlation (i.e. one that correlates the core and accounts for essentially all of the valence correlation energy).

The last application that we discuss that has a strong coupling between the one- and n-particle spaces is the calculation of the electron affinities (EAs) of atomic oxygen (52) and fluorine (29). We have noted earlier for OH and $F+H_2$ that extra orbitals have to be added to the CASSCF active space to describe the negative ion character. The determination of accurate EAs is difficult because the negative ions have more correlation energy than the neutrals and the correlation effects are different. The one-particle requirements are also greater for the negative ions in that the basis sets must be augmented with diffuse functions. For example, in O/O^- if only the $2p$ electrons are correlated, improving the level of treatment from

an SCF/SDCI to a CASSCF/MRCI that includes the $2p$ and $2p'$ orbitals in the active space increases the EA from 1.06 to 1.26 eV. Further expansion of the active space, to include the $3d$ orbital, increases the EA by only 10% of the effect of adding the $2p'$. When the $2s$ and $2p$ electrons are correlated, the change in the EA is even larger when the $2p'$ orbital is added to the active space, from 0.99 at the SCF/SDCI level to 1.28 eV at the CASSCF/MRCI level. In fact, at the SDCI level the inclusion of $2s$ correlation *decreases* the EA, while at the CASSCF/MRCI level $2s$ correlation increases it. It is highly likely that the effect of adding the $3d$ orbital to the active space will increase when both $2s$ and $2p$ correlation are included. Thus, there is a strong coupling between the importance of $2s$ correlation and the level of correlation treatment. Less extensive studies on F/F^- suggest that the +Q correction helps in accounting for this $2s$ effect, but large reference spaces are still required. The dimension of the n-particle problem is further increased by the fact that tight thresholds must be employed in selecting the reference space based on the CASSCF wave functions to avoid significant discrepancies with the unselected CAS reference space MRCI. Thus the study of atomic EAs indicate that as molecular systems become increasingly ionic, larger theoretical treatments are required to obtain equivalent accuracy for the neutral and ion.

For the three applications discussed in this section, the FCI benchmark calculation as well as the CASSCF/MRCI calculations in the large basis sets have given insight into the reason why such extensive calculations are required. Unfortunately, this level of treatment is not routinely possible. It is possible that a CV operator approach (184) will allow the inclusion of this effect without greatly expanding the calculation. Since the +Q correction appears to improve the results for the systems considered in this section, it is also possible that improved methods of estimating the higher excitations will eliminate the need to expand the zeroth-order valence treatment over that which is required for only the valence correlation.

XI. CONCLUSIONS

The cumulative experience derived from FCI benchmark calculations indicates that the more sophisticated n-particle space treatments in use, particularly the CASSCF/MRCI method, generally provide a close approximation to the solution of the correlation problem. In cases in which bonds are not broken, or excited states are not considered, in light atom molecules, single-reference-based treatments of

exact or approximate coupled-cluster type also generate high-quality wave functions. With current supercomputers it is perfectly feasible to consider CC or MRCI expansions of more than 10^6 terms, which opens up large areas of chemistry and spectroscopy to accurate investigation. Indeed, the main factor that determines the accuracy of such treatments is the completeness of the one-particle space. Although there has been justifiable pessimism in the past about the slow convergence towards basis set completeness with respect to both radial saturation and angular quantum number, recent developments in optimized basis sets, particularly the use of atomic natural orbital contractions, have shown that results of full chemical accuracy (better than 1 kcal/mole even in the dissociation energy of N_2) can be achieved with manageable basis sets and reasonable MRCI expansions.

In this review we have shown how FCI benchmark calculations can be used not only to provide general criteria by which approximate n-particle space treatments can be judged, but also to provide detailed calibration as to which treatments are appropriate in specific cases. In this way it is possible to attach confidence limits to the computed results obtained when such a treatment is applied in a large ANO basis. This ability to estimate realistic "error bars" for calculated quantities is very important when the results are to be used in interpreting experiment or in other calculations, and we can expect more use to be made of it in the future. We have described several applications of this technique to problems in spectroscopy (such as the D_e values for NH and CN) and chemistry ($F+H_2$ barrier height).

For the future, there is reason for considerable optimism about the methodology and application of accurate quantum chemistry. A new generation of FCI programs should increase the size of FCI benchmark calculations by more than an order of magnitude, while the constant advances in more conventional methodologies, even in areas thought to be exhausted, will continue. Further, new methods, particularly the application of multireference coupled-cluster approaches, can be expected to find wider use, and some of the more exotic techniques that are currently being explored may begin to contribute to meaningful chemical applications. When combined with the wider availability and increasing power of supercomputers and minisupercomputers, the prospects for accurate quantum chemical calculations look bright indeed.

Acknowledgements

We would like to thank P. J. Knowles and N. Handy for giving us the original version of the FCI code. We would also like to acknowledge collaborations with the groups in Lund (B. O. Roos), Minneapolis (J. Almlöf) and Stockholm (P. E. M. Siegbahn). In addition, a number of our colleagues at NASA-Ames have contributed to this work. We would like to especially thank L. A. Barnes, T. J. Lee, H. Partridge, and D. W. Schwenke. The authors would also like to thank the NAS facility for access to the CRAY-2 and CRAY Y-MP, and to the Central Computing Facility for access to the CRAY X-MP/14se. Finally, we are grateful to the Journal of Chemical Physics for permission to reproduce Figs. 1-3.

REFERENCES

1. *Advances in Chemical Physics: Ab initio methods in quantum chemistry* (Ed. K. P. Lawley), Vol. 67 and 69, Wiley, New York, 1987.

2. McIsaac, K. and Maslen, E. N., *Int. J. Quantum Chem.*, **31**, 361 (1987), and references therein.

3. Löwdin, P. O., *Adv. Chem. Phys.*, **2**, 207 (1959).

4. Bartlett, R. J., *Ann. Rev. Phys. Chem.*, **32**, 359 (1981).

5. Pople, J. A., Binkley, J. S., and Seeger, R., *Int. J. Quantum Chem. Symp.*, **10**, 1 (1976).

6. McLean, A. D. and Liu, B., *J. Chem. Phys.*, **58**, 1066 (1973).

7. Bobrowicz, F. W. and Goddard, W. A. in *Methods of Electronic Structure Theory* (Ed. H. F. Schaefer), p. 79, Plenum Press, New York, 1977.

8. Roos, B. O., *Adv. Chem. Phys.*, **69**, 399 (1987).

9. Docken, K. K. and Hinze, J., *J. Chem. Phys.*, **57**, 4928 (1972).

10. Siegbahn, P. E. M., *Int. J. Quantum Chem.*, **23**, 1869 (1983).

11. Werner, H-J. and Knowles, P. J., *J. Chem. Phys.*, **89**, 5803 (1988).

12. Langhoff, S. R. and Davidson, E. R., *Int. J. Quantum Chem.*, **8**, 61 (1974).

13. Blomberg, M. R. A. and Siegbahn, P. E. M., *J. Chem. Phys.*, **78**, 5682 (1983).

14. Bartlett, R. J., Shavitt, I. and Purvis, G. D., *J. Chem. Phys.*, **71**, 281 (1979), where the addition of the +Q correction was shown to significantly increase the standard deviation for the fitted potential.

15. Ahlrichs, R., *Comput. Phys. Commun.*, **17**, 31 (1979).

16. Cizek, J., *J. Chem. Phys.*, **45**, 4256 (1966).

17. Ahlrichs, R., Scharf, P. and Ehrhardt, C., *J. Chem. Phys.*, **82**, 890 (1985).

18. Gdanitz, R. J. and Ahlrichs, R., *Chem. Phys. Lett.*, **143**, 413 (1988).

19. Helgaker, T. and Jørgensen, P., *Adv. Quantum Chem.*, **19**, 183 (1988).

20. Chong, D. P. and Langhoff, S. R., *J. Chem. Phys.*, **84**, 5606 (1986).

21. Shavitt, I., in *Methods of Electronic Structure Theory* (Ed. H. F. Schaefer), p. 189, Plenum, New York, 1977.

22. Roos, B. O. and Siegbahn, P. E. M., in *Methods of Electronic Structure Theory* (Ed. H. F. Schaefer), p. 277, Plenum, New York, 1977.

23. Siegbahn, P. E. M., in *Quantum Chemistry: The State of the Art* (Eds. V. R. Saunders and J. Brown), p. 81, Science Research Council, Didcot Oxon., 1975.

24. Handy, N. C., *Chem. Phys. Lett.*, **74**, 280 (1980).

25. Saxe, P., Fox, D. J., Schaefer, H. F. and Handy, N. C., *J. Chem. Phys.*, **77**, 5584 (1982).

26. Siegbahn, P. E. M., *Chem. Phys. Lett.*, **109**, 417 (1984).

27. Downward, M. J. and Robb, M. A., *Theor. Chim. Acta.*, **46**, 129 (1977).

28. Knowles, P. J. and Handy, N. C., *Chem. Phys. Lett.*, **111**, 315 (1984).

29. Bauschlicher, C. W. and Taylor, P. R., *J. Chem. Phys.*, **85**, 2779 (1986).

30. Davidson, E. R., *J. Comput. Phys.*, **17**, 87 (1975).

31. Olsen, J. Roos, B O., Jørgensen, P., and Jensen, H. J., *J. Chem. Phys.*, **89**, 2185 (1988).

32. Bauschlicher, C. W. and Taylor, P. R., *J. Chem. Phys.*, **86**, 2844 (1987).

33. Malmquist, P-Å., Rendell, A. P., and Roos, B. O., private communication.

34. Knowles, P. J., *Chem. Phys. Lett.* (in press).

35. Knowles, P. J. and Handy, N. C., to be published.

36. Harrison, R. J., and Zarrabian, S., private communication.

37. Siegbahn, P. E. M. and Liu, B., *J. Chem. Phys.*, **68**, 2457 (1978).

38. Bauschlicher, C. W., *J. Phys. B,* **21**, L413 (1988).

39. Harcourt, R. D., *J. Phys. B,* **20**, L617 (1987).

40. Taylor, P. R., Bauschlicher, C. W., and Langhoff, S. R., *J. Phys. B,* **21**, L333 (1988).

41. Garton, W. R. S., in *Proceedings of the Fifth Conference on Ionization Phenomena in Gases, 1961* p. 1884 Amsterdam: North-Holland, 1962.

42. Eriksson, K. B. S. and Isberg, I. B. S., *Arkiv Fysik,* **23**, 527 (1963).

43. Weiss, A. W., *Adv. At. Mol. Phys.,* **9**, 1 (1973).

44. Weiss, A. W., *Phys. Rev. A,* **9**, 1524 (1974).

45. Saxe, P., Schaefer H. F., and Handy, N. C., *Chem. Phys. Lett.,* **79**, 202 (1981).

46. Harrison, R. J. and Handy, N. C., *Chem. Phys. Lett.,* **96**, 386 (1983).

47. Bartlett, R. J., Sekino, H., and Purvis, G. D., *Chem. Phys. Lett.,* **98**, 66 (1983).

48. Laidig, W. D. and Bartlett, R. J., *Chem. Phys. Lett.,* **104**, 424 (1984).

49. Brown, F. B., Shavitt, I., and Shepard, R., *Chem. Phys. Lett.,* **105**, 363 (1984).

50. Bauschlicher, C. W., Langhoff, S. R., Taylor, P. R., and Partridge, H., *Chem. Phys. Lett.,* **126**, 436 (1986).

51. Bauschlicher, C. W., Langhoff, S. R., Taylor, P. R., Handy, N. C., and Knowles, P. J., *J Chem. Phys.*,**85**, 1469 (1986).

52. Bauschlicher, C. W., Langhoff, S. R., Partridge, H., and Taylor, P. R., *J. Chem. Phys.,* **85**, 3407 (1986).

53. Bauschlicher, C. W. and Taylor, P. R., *J. Chem. Phys.,* **85**, 6510 (1986).

54. Bauschlicher, C. W. and Taylor, P. R., *J. Chem. Phys.,* **86**, 1420 (1987).

55. Bauschlicher, C. W. and Taylor, P. R., *J. Chem. Phys.,* **86**, 858 (1987).

56. Bauschlicher, C. W. and Taylor, P. R., *Theor. Chim. Acta*, **71**, 263 (1987).

57. Bauschlicher, C. W. and Taylor, P. R., *J. Chem. Phys.*, **86**, 5600 (1987).

58. Bauschlicher, C. W., *J. Chem. Phys.*, **86**, 5591 (1987).

59. Bauschlicher, C. W. and Langhoff, S. R., *J. Chem. Phys.*, **86**, 5595 (1987).

60. Bauschlicher, C. W. and Langhoff, S. R., *Chem. Phys. Lett.*, **135**, 67 (1987).

61. Langhoff, S. R., Bauschlicher, C. W., and Taylor, P. R., *J. Chem. Phys.*, **86**, 6992 (1987).

62. Bauschlicher, C. W., Partridge, H., Langhoff, S. R., Taylor, P. R., and Walch, S. P. *J. Chem. Phys.*, **86**, 7007 (1987).

63. Bauschlicher, C. W. and Langhoff, S. R., *J. Chem. Phys.*, **87**, 4665 (1987).

64. Bauschlicher, C. W. and Langhoff, S. R., *Theor. Chim. Acta*, **73**, 43 (1988).

65. Bauschlicher, C. W., *J. Phys. Chem.*, **92**, 3020 (1988).

66. Bauschlicher, C. W., Langhoff, S. R., and Taylor, P. R., *J. Chem. Phys.*, **88**, 2540 (1988).

67. Bauschlicher, C. W., Langhoff, S. R., Partridge, H., and Chong, D. P. *J. Chem. Phys.*, **89**, 2985 (1988).

68. Bauschlicher, C. W. and Langhoff, S. R., *J. Chem. Phys.*, **89**, 2116 (1988).

69. Bauschlicher, C. W. and Langhoff, S. R., *J. Chem. Phys.*, **89**, 4246 (1988).

70. Taylor, P. R., Komornicki, A., and Dixon, D. A., *J. Am. Chem. Soc.*, (in press).

71. Bauschlicher, C. W. and Langhoff, S. R., *J. Chem. Phys.*, **87**, 2919-2924.

72. Cole, S. J. and Bartlett, R. J., *J. Chem. Phys.*, **86**, 873 (1987).

73. Murrell, J. N., Hassian, N. M. R., and Hudson, B., *Mol. Phys.*, **60**, 1343 (1987).

74. Jankowski, K., Becherer, R., Scharf, P., Schiffer, H., and Ahlrichs, R., *J. Chem. Phys.*, **82**, 1413 (1985).

75. Blomberg, M. R. A. and Siegbahn, P. E. M., *Chem. Phys. Lett.*, **81**, 4 (1981).

76. Lengsfield, B. H., McLean, A. D., Yoshimine, M., and Liu, B., *J. Chem. Phys.*, **79**, 1891 (1983).

77. Dunning T. H. and Hay, P. J. in *Methods of Electronic Structure Theory* (Ed. H. F. Schaefer), p. 1, Plenum Press, New York, 1977.

78. Raffenetti, R. C., *J. Chem. Phys.*, **58**, 4452 (1973).

79. Shavitt, I., Rosenberg, B. J., and Palalikit, S., *Int. J. Quantum Chem. Symp.*, **10**, 33 (1976).

80. Almlöf, J. and Taylor, P. R., *J. Chem. Phys.*, **86**, 4070 (1987).

81. Boys, S. F. and Bernardi, F., *Mol. Phys.*, **19**, 553 (1970).

82. Liu, B. and McLean, A. D., *J. Chem. Phys.*, **59**, 4557 (1973).

83. Langhoff, S. R., Bauschlicher, C. W., and Taylor, P. R., *J. Chem. Phys.*, **88**, 5715 (1988).

84. Almlöf, J., Helgaker, T. U., and Taylor, P. R., *J. Phys. Chem.*, **92**, 3029 (1988).

85. Bauschlicher, C. W., *Chem. Phys. Lett.*, **142**, 71 (1987).

86. Dunning, T. H., *J. Chem. Phys.*, **90**, 1007 (1989).

87. Ahlrichs, R. Jankowski, K. and Wasilewski, J., *Chem. Phys.*, **111**, 263 (1987).

88. Bauschlicher, C. W., Langhoff, S. R., and Taylor, P. R., *J. Chem. Phys.*, **87**, 387 (1987).

89. Werner, H.-J. and Reinsch, E.-A., in *Proceedings of the 5th European seminar on computational methods in quantum chemistry* (Eds. P. Th. van Duijnen and W. C. Nieuwpoort), p. 206 Max-Planck-Institut für Astrophysik, Munich, 1981.

90. McLean, A. D., Bunker, P. R., Escribano, R. M., and Jensen, P., *J. Chem. Phys.*, **87**, 2166 (1987).

91. Handy, N. C., Yamaguchi, Y., and Schaefer, H. F., *J. Chem. Phys.*, **84**, 4481 (1986).

92. Cowan, R. D. and Griffin, D. C., *J. Opt. Soc. Am.*, **66**, 1010 (1976).

93. Martin, R. L., *J. Phys. Chem.*, **87**, 750 (1983).

94. Krauss, M. and Stevens, W. J., *Ann. Rev. Phys. Chem.*, **35**, 5357 (1984).

95. Allen, W. D. and Schaefer, H. F., *Chem. Phys.*, **108**, 243 (1986).

96. Berkowitz, J., Greene, J. P., Cho, H., and Ruscic, B., *J. Chem. Phys.*, **86**, 1235 (1987).

97. Balasubramanian K. and McLean, A. D., *J. Chem. Phys.*, **85**, 5117 (1986).

98. Basch, H., Stevens, W. J., and Krauss, M., *Chem. Phys. Lett.*, **109**, 212 (1984).

99. Sunil, K. K. and Jordan, K. D., *J. Phys. Chem.*, **92**, 2774 (1988).

100. Leleyter, M. and Joyce, P., *J. Phys. B*, **13**, 2165 (1980).

101. Upton, T. H., *J. Phys. Chem.*, **90**, 754 (1986).

102. Cox, D. M., Trevor, D. J., Whetten, R. L., Rohlfing, E. A., and Kaldor, A., *J. Chem. Phys.*, **84**, 4651 (1986).

103. Douglas, M. A., Hauge, R. H., and Margrave, J. L., *J. Phys. Chem.*, **87**, 2945 (1983).

104. Abe, H. and Kolb, D. M., *Ber. Bunsenges. Phys. Chem.*, **87**, 523 (1983).

105. Ginter, D. S., Ginter, M. L., and Innes, K. K., *Astrophys. J.*, **139**, 365 (1963)

106. Fu, Z., Lemire, G. W., Hamrick, Y. M., Taylor, S., Shui, J., and Morse, M. D., *J. Chem. Phys.*, **88**, 3524 (1988).

107. Cai, M. F., Dzugan, T. P., and Bondybey, V. E., to be published.

108. Huber, K. P., and Herzberg, G. *Constants of Diatomic Molecules,* Van Nostrand Reinhold, New York, 1979.

109. Taylor, P. R. and Partridge, H., *J. Phys. Chem.*, **91**, 6148 (1987).

110. Meinel, A. B., *J. Astrophys.*, **11**, 555 (1950).

111. Langhoff, S. R., Jaffe, R. L., Yee, J. H., and Dalgarno, A., *Geophysical Research Lett.*, **10**, 896 (1983).

112. Yaron, D., Peterson, K., and Klemperer, W., *J. Chem. Phys.*, **88**, 4702 (1988).

113. Werner, H.-J. and Rosmus, P., in *Comparison of Ab Initio Quantum Chemistry with Experiment* (Ed. R. Bartlett.), p. 267 D. Reidel Publishing Company, Boston, 1985.

114. Oddershede, J., *Phys. Scr.*, **20**, 587 (1979).

115. German, K. R., Bergeman, T. H., Weinstock, E. M., and Zare, R. N., *J. Chem. Phys.*, **58**, 4304 (1973) and references therein.

116. Brzozowski, J., Erman, P., and Lyyra, M., *Phys. Scr.*, **17**, 507 (1978).

117. Dimpfl, W. L. and Kinsey, J. L., *J. Quant. Spectrosc. Radiat. Transf.*, **21**, 233 (1979).

118. German, K. R., *J. Chem. Phys.*, **64**, 4065 (1976).

119. McDermid, I. S. and Laudenslager, J. B., *J. Chem. Phys.*, **76**, 1824 (1982).

120. Matos, J. M. O., Malmqvist, P-Å., and Roos, B. O., *J. Chem. Phys.*, **86**, 5032 (1987).

121. Meyer, W. and Rosmus, P., *J. Chem. Phys.*, **63**, 2356 (1975).

122. Piper, L. G., *J. Chem. Phys.*, **70**, 3417 (1979).

123. Chase, M. W., Curnutt, J. L., Downey, J. R., McDonald, R. A., Syverud, A. N, and Valenzuela, E. A., *J. Phys. Chem. Ref. Data*, **11**, 695 (1982).

124. Graham, W. R. and Lew, H., *Can. J. Phys.*, **56**, 85 (1978).

125. Hofzumahaus, A. and Stuhl, F., *J. Chem. Phys.*, **82**, 5519 (1985).

126. Ervin, K. M. and Armentrout, P. B., *J. Chem. Phys.*, **86**, 2659 (1987).

127. Langhoff, S. R., Bauschlicher, C. W., and Taylor, P. R., *Chem. Phys. Lett.*, **135**, 543 (1987).

128. Liu, B., private communication.

129. Almlöf, J., Taylor, P. R., Bauschlicher, C. W., and Siegbahn, P. E. M., unpublished.

130. Sneden, C. and Lambert, D. L., *Astrophys. J.*, **259**, 381 (1982).

131. Bauschlicher, C. W., Langhoff, S. R., and Taylor, P. R., *Astrophys. J.*, **332**, 531 (1988).

132. Hotop, H. and Lineberger, W. C., *J. Phys. Chem. Ref. Data*, **14**, 735 (1985).

133. Berkowitz, J., Chupka, W. A., and Walter, T. A., *J. Chem. Phys.*, **50**, 1497 (1968).

134. Langhoff, S. R., Bauschlicher, C. W., and Partridge, H., *J. Chem. Phys.*, **87**, 4716 (1987).

135. Langhoff, S. R. and Bauschlicher, C. W., *J. Chem. Phys.*, **88**, 329 (1988).

136. Duric, N. Erman P., and Larsson, M., *Phys. Scr.*, **18** 39 (1978).

137. Peterson, J. R. and Moseley, J. T., *J. Chem. Phys.*, **58**, 172 (1973).

138. Johnson, A. W. and Fowler, R. G., *J. Chem. Phys.*, **53**, 65 (1970).

139. Cartwright, D. C. and Hay, P. J., *Astrophys. J.*, **257**, 383 (1982).

140. Taherian, M. R. and Slanger, T. G., *J. Chem. Phys.*, **81**, 3814 (1984).

141. Arnold, J. O. and Nicholls, R. W., *J. Quant. Spectrosc. Radiat. Transf.*, **12**, 1435 (1972).

142. Davis, S. P., Shorenhaus, D., Stark, G., Engleman, R., Phillips, J. G., and Hubbard, R. P., *Astrophys. J.*, **303**, 892 (1986).

143. Zucconi, J. M., and Festou, M. C., *Astron. Astrophys.*, **150**, 180 (1985).

144. Treffers, R. R., *Astrophys. J.*, **196**, 883 (1975).

145. Langhoff, S. R. and Bauschlicher, C. W., *Astrophys. J.*, (in press).

146. Anketell, J. and Nicholls, R. W., *Rep. Prog. Phys.*, **33**, 269 (1970).

147. Berkowitz, J., Chupka, W. A., and Kistiakowsky, G. B., *J. Chem. Phys.* **25**, 457 (1956).

148. Campbell, I. M. and Thrush, B. A., *Proc. Roy. Soc.* **A296**, 201 (1967).

149. Carroll, P. K., *J. Chem Phys.*, **37**, 805 (1962).

150. Partridge, H., Langhoff, S. R., Bauschlicher, C. W., and Schwenke, D. W., *J. Chem. Phys.*, **88**, 3174 (1988).

151. Carroll, P. K. and Sayers, N. P., *Proc. Phys. Soc. London Sect.* **A66**, 1138 (1953).

152. Nadler, I. and Rosenwaks, S., *J. Chem. Phys.*, **83**, 3932 (1985).

153. Huber, K. P. and Vervloet, M., *J. Chem. Phys.*, **89**, 5957 (1988).

154. Langhoff, S. R. and Bauschlicher, C. W., *Ann. Rev. Phys. Chem.*, **39**, 181 (1988).

155. Moore, C. E. (1949), *Atomic energy levels US Natl. Bur. Stand. (US)*, circ. no. 467.

156. Gray, J. A., Rice, S. F., and Field, R. W., *J. Chem. Phys.*, **82**, 4717 (1985).

157. Walch, S. P., Bauschlicher, C. W., and Langhoff, S. R., *J. Chem. Phys.*, **83**, 5351 (1985).

158. McLean, A. D. and Liu, B., to be published.

159. Partridge, H., *J. Chem. Phys.*, **90**, 1043 (1989).

160. Stevens, A. E., Feigerle, C. S., and Lineberger, W. C., *J. Chem. Phys.*, **78**, 5420 (1983).

161. Balfour, W. J., Lindgren, B., and O'Connor, S., *Phys. Scr.*, **28** 551 (1983).

162. Walch, S. P., *Chem. Phys. Lett.*, **105**, 54 (1984).

163. Bauschlicher, C. W. and Langhoff, S. R., *Chem. Phys. Lett.*, **145**, 205 (1988).

164. See for example the volume of Chem. Rev. (and references therein) devoted to Chemical Dynamics; *Chem. Rev.*, **87**, (1987).

165. Lifshitz, A., Bidani, M. and Carroll, H. F., *J. Chem. Phys.*, **79**, 2742 (1983).

166. Lohr, L. L., *Chem. Phys. Lett.*, **56**, 28 (1978) and references therein.

167. Dixon, D. A., Stevens, R. M., and Herschbach, D. R., *Far. Disc. Chem. Soc.*, **62**, 110 (1977).

168. Bauschlicher, C. W., Walch, S. P., Langhoff, S. R., Taylor, P. R., and Jaffe, R. L., *J. Chem. Phys.*, **88**, 1743 (1988).

169. Bauschlicher, C. W., Langhoff, S. R., Lee, T. J., and Taylor, P. R., *J. Chem. Phys.*, in press.

170. Frisch, M. J., Liu, B., Binkley, J. S., Schaefer, H. F., and Miller, W. H., *Chem. Phys. Lett.*, **114**, 1 (1985).

171. Steckler, R., Schwenke, D. W., Brown, F. B., and Truhlar, D. G., *Chem.*

Phys. Lett. **121**, 475 (1985); Schwenke, D. W., Steckler, R., Brown, F. B., and Truhlar, D. G., *J. Chem. Phys.*, **84**, 5706 (1986); Schwenke, D. W., Steckler, R., Brown, F. B., and Truhlar, D. G., *J. Chem. Phys.*, **86**, 2443 (1987).

172. Garmer, D. R. and Anderson, J. B., *J. Chem. Phys.*, **89**, 3050 (1988).

173. Scuseria, G. E. and Schaefer, H. F., *J. Chem. Phys.*, **88**, 7024 (1988).

174. Schaefer, H. F., *J. Phys. Chem.*, **89**, 5336 (1985) and references therein.

175. Neumark, D. M., Wodtke, A. M., Robinson, G. N., Hayden, C. C., and Lee, Y. T., *J. Chem. Phys.*, **82**, 3045 (1985).

176. Neumark, D. M., Wodtke, A. M., Robinson, G. N., Hayden, C. C., Shobatake, K., Sparks, R. K., Schafer, T. P., and Lee, Y. T., *J. Chem. Phys.*, **82**, 3067 (1985).

177. Garrett, B. C., Truhlar, D. G., Grev, R. S., and Magnuson, A. W., *J. Phys. Chem.*, **84**, 1730 (1980).

178. Desouter-Lecomte, M., Leclerc, J. C., and Lorquet, J. C., *J. Chem. Phys.*, **66**, 4006 (1977).

179. Grice, R. and Herschbach, D. R., *Mol. Phys.*, **27**, 159 (1974).

180. Kahn, L. R., Hay, P. J., and Shavitt, I., *J. Chem. Phys.*, **61**, 3530 (1974).

181. Lengsfield, B. H., Saxe, P., and Yarkony, D. R., *J. Chem. Phys.*, **81**, 4549 (1984).

182. Saxe, P., Lengsfield, B. H., and Yarkony, D. R., *Chem. Phys. Lett.*, **113**, 159 (1985).

183. Werner, H.-J. and Meyer, W., *J. Chem. Phys.*, **74**, 5802 (1981).

184. Müller, W., Flesch, J. and Meyer, W., *J. Chem. Phys.*, **80**, 3297 (1984).

185. Knight, L. B., Johannessen, K. D., Cobranchi, D. C., Earl, E. A., Feller, D., and Davidson, E. R., *J. Chem. Phys.*, **87**, 885 (1987).

Table I. $^1A_1 - {}^3B_1$ separation in CH_2 (kcal/mole) using a DZP basis set and correlating the six valence electrons.

Method	Separation	Error
SCF[a]	26.14	14.17
SCF[a]/SDCI	14.63	2.66
SCF/SDCI+Q	12.35	0.38
CPF	12.42	0.45
TCSCF[b]/MRCI	12.20	0.23
TCSCF/MRCI+Q	12.03	0.06
CASSCF[c]/MRCI	11.97	0.00
CASSCF/MRCI+Q	11.79	−0.18
FCI	11.97	—

[a] The SCF occupations are $1a_1^2 2a_1^2 3a_1^2 1b_2^2$ and $1a_1^2 2a_1^2 1b_2^2 3a_1^1 1b_1^1$.

[b] SCF treatment for $^3B_1$ state, two-configuration MCSCF treatment for $^1A_1$ state (SCF configuration and $3a_1^2 \rightarrow 1b_1^2$ excitation).

[c] Active space comprises the C $2s$ $2p$ and H $1s$ orbitals .

Table II. Spectroscopic constants for the $^1\Sigma_g^+$ state of N_2.

Method	r_e (a_0)	DZP basis 6 electrons correlated ω_e (cm^{-1})	D_e (eV)
SDCI	2.102	2436	8.298
SDCI+Q	2.115	2373	8.613
SDTCI	2.107	2411	8.462
SDTQCI	2.121	2343	8.732
SDQCI	2.116	2361	8.586
CPF	2.112	2382	8.526
MCPF	2.114	2370	8.556
MRCI	2.123	2334	8.743
MRCI+Q	2.123	2333	8.766
FCI	2.123	2333	8.750

Table III. Polarizability of F^- (a_0^3)

Method	DZP + diffuse *spd* basis 8 electrons correlated, $\alpha = d^2E/dF^2$ α
SDCI	13.965
SDCI+Q	15.540
CPF	16.050
MRCI[a]	16.134
MRCI+Q	16.346
MRCI'[b]	16.034
MRCI'+Q	16.303
FCI	16.295

[a] The MRCI treatment is a CAS reference CI based on a CASSCF calculation that included the $2p$ electrons and the $2p$ and $3p$ orbitals in the active space.
[b] The MRCI treatment is a CAS reference CI based on a CASSCF calculation that included the $2s$ and $2p$ electrons and the $2s$, $2p$, $3s$ and $3p$ orbitals in the active space.

Table IV. $N(^4S)/N_2(^1\Sigma_g^+)$ extended basis total energies (E_H), correlation energies (E_{corr})(E_H) and "dissociation energies" (eV).

N atom

Basis set	$E_{SCF}+54.$	E_{corr}
$(13s\ 8p\ 6d)$	-0.400790	-0.111493
$[6s\ 5p\ 4d]$	-0.400779	-0.111321
$[5s\ 4p\ 3d]$	-0.400769	-0.110925
$[4s\ 3p\ 2d]$	-0.400725	-0.109066
$(13s\ 8p\ 6d\ 4f)$	-0.400790	-0.121385
$[5s\ 4p\ 3d\ 2f]$	-0.400769	-0.120499
$[4s\ 3p\ 2d\ 1f]$	-0.400725	-0.117584
$[5s\ 4p\ 3d\ 2f]\ (2g)^a$	-0.400769	-0.122472
$[5s\ 4p\ 3d\ 2f\ 1g]$	-0.400769	-0.122138

N_2 molecule[b]

Basis set	$E_{SCF}+108.$	E_{corr}	D_e(SCF)	D_e(SDCI)
$(13s\ 8p\ 6d)$	-0.986307	-0.338118	5.03	8.16
$[6s\ 5p\ 4d]$	-0.985913	-0.337304	5.02	8.14
$[5s\ 4p\ 3d]$	-0.984833	-0.335395	4.99	8.08
$[4s\ 3p\ 2d]$	-0.983483	-0.329330	4.95	7.98
$(13s\ 8p\ 6d\ 4f)$	-0.989318	-0.365735	5.11	8.45
$[5s\ 4p\ 3d\ 2f]$	-0.988031	-0.362548	5.07	8.38
$[4s\ 3p\ 2d\ 1f]$	-0.986230	-0.353283	5.03	8.24
$[5s\ 4p\ 3d\ 2f\ ](2g)^a$	-0.988458	-0.370808	5.09	8.51
$[5s\ 4p\ 3d\ 2f\ 1g]$	-0.988322	-0.369270	5.08	8.48

[a] 2 uncontracted g sets.

[b] $r(\text{N–N}) = 2.1\ a_0$, 10 electrons correlated.

Table V. Theoretical study of the $^1A_1 - {}^3B_1$ separation in CH_2 and SiH_2.

ANO basis set	Separation (kcal/mole)[a]
	CH_2
[3*s* 2*p* 1*d*/2*s* 1*p*]	11.33
[4*s* 3*p* 2*d* 1*f*/3*s* 2*p* 1*d*]	9.66
[5*s* 4*p* 3*d* 2*f* 1*g*/4*s* 3*p* 2*d*]	9.24
Expt+theory (T_e)	9.28 ($\pm$0.1)[b]
Core-Valence	+0.35[c]
Born-Oppenheimer	−0.1[d]
Relativistic	−0.06[a]
	SiH_2
[6*s* 5*p* 1*d*/3*s* 1*p*]	−19.46
[6*s* 5*p* 2*d* 1*f*/3*s* 2*p* 1*d*]	−20.15
[6*s* 5*p* 3*d* 2*f* 1*g*/4*s* 3*p* 2*d*]	−20.29
Relativistic	−0.30
Zero-point	−0.33[e]
Expt(T_0)	−21.0$\pm$0.7[f]

[a] Ref. 88.
[b] Ref. 90.
[c] Ref. 56.
[d] Ref. 91.
[e] Ref. 95.
[f] Ref. 96.

Table VI. Summary of the D_0 values for the $X^3\Sigma^-$ state of NH, in eV.

	CH	NH	OH
MRCI[a]	3.433	3.344	4.360
Recommended[a]		3.37±0.03	
Experiment[b]	3.465	>3.29	4.393
		<3.47	

[a] Ref. 60.

[b] Refs. 108, 124 and 125.

Table VII. Spectroscopic constants for the $^1\Sigma_g^+$ state of N_2.

	[5*s* 4*p* 3*d* 2*f* 1*g*] basis		
Method	r_e (Å)	ω_e (cm^{-1})	D_e (eV)
MRCI(6)	1.096	2382	10.015
MRCI(6)+Q	1.096	2382	10.042
MRCI(10)	1.101	2343	9.723
MRCI(10)+Q	1.102	2336	9.745
Expt[a]	1.098	2359	9.905

[a] Ref. 108.

Table VIII. Band positions and relative intensities of the HIR system of N_2.

Band	Band positions (nm)		Relative intensities	
	Theory	Experiment[a]	Theory	Experiment[a]
0-0	806[b]	806	3.5	4.0
0-1	854	855	1.0[c]	1.0
0-2	906	907	0.6	
0-3	960	963	0.3	
0-4	1016	1023	0.1	
1-0	753	752	6.0[c]	6.0
1-1	795	795	0.2	
1-2	840	840	0.7	<0.5
1-3	885	887	1.6	
1-4	932	938	1.4	
2-0	707	706	10.0[c]	10.0
2-1	745	744	8.8	8.0
2-2	783	783	6.6	5.0
2-3	823	824	0.3	<0.5
2-4	864	868	0.7	
3-0	668	667	1.5[c]	1.5
3-1	701	700	10.4	9.0
2-3	735	735	0.6	<0.5
3-3	771	771	4.8	3.0
3-4	806	809	2.5	

[a]Ref. 152.

[b]The 0-0 bands were shifted into coincidence; this required a shift of 567 cm^{-1} in the theoretical T_e.

[c]These bands were normalized to experiment by adjusting the vibrational populations. This requires that the relative populations of v'=0-3 be 0.073, 0.295, 1.00, and 0.725, respectively.

Table IX. FCI calibration of the classical barrier height of $F+H_2 \rightarrow HF+H$[a].

A. At the FCI saddle point

	barrier	exothermicity
FCI	4.50	28.84
MRCI(300)	5.18	28.57
MRCI(300)+Q	4.43	29.12
MRCI(322)(0.05)	5.00	29.12
MRCI(322)(0.05)+Q	4.32	29.21
MRCI(322)(0.025)[b]	4.73	29.17
MRCI(322)(0.025)+Q[b]	4.51	28.80
ACPF(322)(0.025)(12-Ref)[b]	4.56	28.89
ACPF(322)(0.025)(13-Ref)[c]	4.57	28.89
MRCI(322)(0.01)	4.71	29.19
MRCI(322)(0.01)+Q	4.54	28.84
MRCI(522)(0.025)	4.55	29.41
MRCI(522)(0.025)+Q	4.32	29.31

B. At the optimized saddle-point geometry[d]

	r(F-H)	r(H-H)	ΔE_b	ΔE_{rx}
FCI	2.761	1.467	4.50	28.84
MRCI(300)	2.740	1.476	5.16	28.57
CPF	2.801	1.467	4.40	26.47
MRCI(300)+Q	2.795	1.467	4.42	29.12
MRCI(322)(0.025)[b]	2.761	1.474	4.70	29.17
MRCI(322)(0.025)+Q[b]	2.755	1.475	4.49	28.80
ACPF(322)(0.025)[c]	2.760	1.475	4.56	28.89
SDTQCI[e]	2.763	1.465	4.45	

[a] Energies in kcal/mole and bond lengths in a_0. All calculations are done using the [4*s* 3*p* 1*d*/2*s* 1*p*] basis set and correlating seven electrons. The barrier is referenced to $F...H_2(50a_0)$, and the exothermicity is computed using $HF...H(50a_0)$.

[b] The 12 reference configurations chosen from the CASSCF wave function.

[c] Includes the additional configuration found to be important in the ACPF calculation — see the text.

[d] Geometry optimized using a biquadratic fit to a grid of nine points.

[e] Scuseria and Schaefer, Ref. 173.

Table X. Theoretical studies of the classical saddle-point geometry (a_0) and energetics (kcal/mole) for the F+H_2 reaction.

Basis[a]	Level of treatment	r^b_{HF}	r^b_{HH}	barrier[c]	exothermicity[c]
12-Ref[d]					
A	MRCI(322)(2p)[e]	2.899	1.455	2.99	33.96
A	MRCI(322)(2p)+Q	2.910	1.456	2.42	33.42
A	MRCI(322)(2p)	(2.95)	(1.45)	2.96	
A	MRCI(322)(2p)+Q	(2.95)	(1.45)	2.40	
A	ACPF(322)(2p)	(2.95)	(1.45)	2.45	
A	MRCI(322)	2.914	1.451	2.63	31.61
A	MRCI(322)+Q	2.950	1.450	1.66	30.47
A	ACPF(322)	(2.95)	(1.45)	1.17	
A	CCI(322)	...[f]	...[f]	2.79	31.8
A	CCI(322)+Q	...[f]	...[f]	2.02	30.7
A+H(f)[g]	CCI(322)	...[f]	...[f]	2.73	
A+H(f)	CCI(322) +Q	...[f]	...[f]	1.95	
A−F(g)	CCI(322)	2.879	1.447	2.89	
A−F(g)	CCI(322)+Q	2.909	1.445	2.14	
13-Ref[h]					
A	MRCI(322)(2p)	(2.95)	(1.45)	2.96	33.96
A	MRCI(322)(2p)+Q	(2.95)	(1.45)	2.51	33.42
A	ACPF(322)(2p)	2.914	1.453	2.61	33.54
A	MRCI(322)	(2.95)	(1.45)	2.59	31.61
A	MRCI(322)+Q	(2.95)	(1.45)	1.81	30.47
A	ACPF(322)	2.967	1.447	1.85	30.58
Expt.[i]					31.73

[a] "A" denotes the [5s 5p 3d 2f 1g/4s 3p 2d] basis described in Ref. 168.

[b] The saddle-point geometries in parentheses have not been optimized.

[c] The barrier is referenced to F...H_2($50a_0$), and the exothermicity is computed using HF...H($50a_0$).

[d] The 12 reference configurations chosen from the CASSCF wave function.

[e] (2p) indicates a seven-electron treatment (i.e. 2s correlation is excluded).

[f] The MRCI(300)+Q saddle point geometry is used, r(F-H)=2.921 a_0 and r(H-H)=1.450 a_0.

[g] Denotes that a function of this angular momentum type has been added.

[h] Includes the additional configuration found to be important in the ACPF calculation — see the text.

[i] From data in Ref. 108.

Table XI. Study of the 2s effect on the $F+H_2$ barrier height(kcal/mole)[a] in the $DZ+p_F$ basis set.

Level of treatment	MRCI	MRCI+Q	ACPF	SDTQCI	FCI
7 electron	8.78	8.74	8.75	8.82	8.77
9 electron	6.68	6.50	6.53	6.82	6.64
Δ	2.10	2.24	2.22	2.00	2.13

[a] The saddle point geometries are taken from the MRCI(2p)+Q and MRCI+Q calculations in this basis set.

Table XII. Zero-point and tunnelling effects on the barrier height of the F + H_2 and F + D_2 reactions.

F + H_2 surface

	Classical Barrier		Adiabatic Barrier	
	CCI	CCI + Q	CCI	CCI + Q
r_{HF}, a_0	2.879	2.909	3.070	3.155
r_{HH}, a_0	1.447	1.445	1.425	1.421
Barrier, kcal/mole	2.888	2.143	2.639	1.860
Sym. stretch, cm^{-1}	3706	3768	4074	4178
Bend, cm^{-1}	68.5	45.9	68.5	45.9
Asym. stretch[a], cm^{-1}	$692i$	$605i$	$530i$	$371i$
Zero-point correction[b], kcal/mole	−0.602	−0.643	−0.076	−0.057
E barrier + zero point, kcal/mole	2.286	1.500	2.563	1.803
Tunnelling correction, kcal/mole	−0.54	−0.47	−0.42	−0.29
Threshold, kcal/mole	1.75	1.03	2.14	1.51

F + D_2 surface

	Classical Barrier		Adiabatic Barrier	
	CCI	CCI + Q	CCI	CCI + Q
r_{HF}, a_0	2.879	2.909	3.010	3.075
r_{HH}, a_0	1.447	1.445	1.430	1.427
Barrier, kcal/mole	2.888	2.143	2.761	1.997
Sym. stretch, cm^{-1}	2623	2667	2811	2876
Bend, cm^{-1}	37.7	19.1	37.7	19.1
Asym. stretch[a], cm^{-1}	$512i$	$448i$	$428i$	$334i$
Zero-point correction[b], kcal/mole	−0.488	−0.532	−0.220	−0.233
E barrier + zero point, kcal/mole	2.400	1.611	2.541	1.764
Tunnelling correction, kcal/mole	−0.40	−0.35	−0.34	−0.26
Threshold, kcal/mole	2.00	1.26	2.20	1.50

[a]From the normal mode analysis at the classical barrier, and computed from the curvature along the Eckart potential at the adiabatic barrier.

[b]For $H_2(D_2)$ we used ω_e=4401(3116) cm^{-1}, respectively, from Ref. 108.

Figure Captions

Figure 1: Comparison of the theoretical radiative lifetimes (63) for different rotational levels of the v=0 level of the $A^2\Sigma^+$ state of OH (dashed line) with the high frequency deflection measurements (F_1 component) of Brzozowski *et al.* (116) shown with error bars.

Figure 2. The FCI potential energy curves for the $X^1\Sigma^+$, $A^1\Pi$, and $C^1\Sigma^+$ states of AlH (68).

Figure 3. Potential energy curves and vibrational levels for the $A^3\Sigma_u^+$, $A'\ ^5\Sigma_g^+$ and $B^3\Pi_g$ states of N_2 (150).

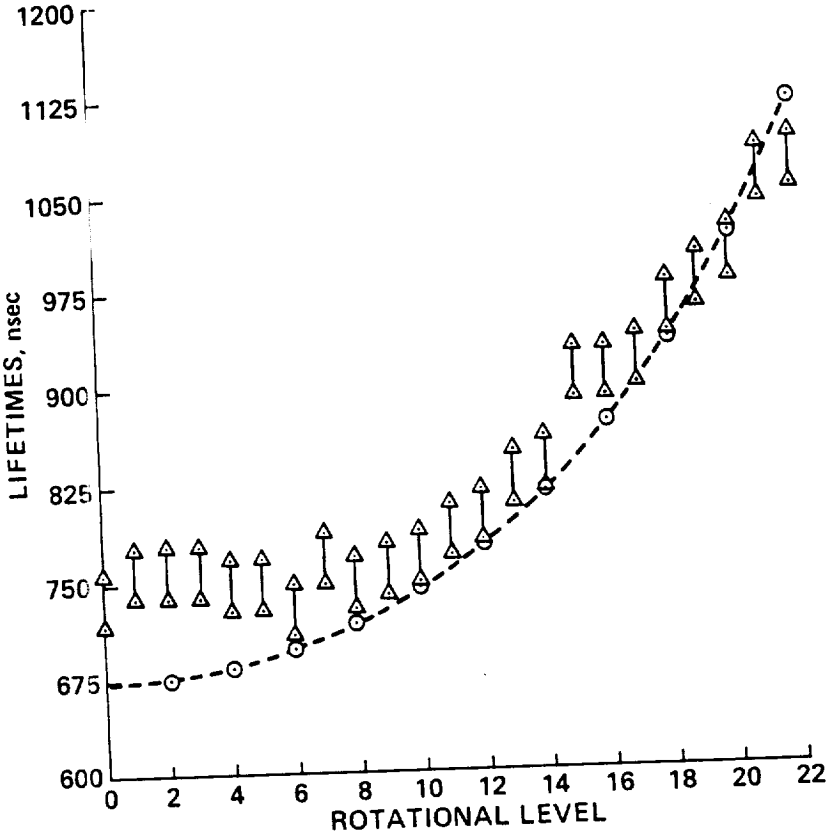
1200
1125
1050
975
900
825
750
675
600
LIFETIMES, nsec
0
2
4
6
8
10
12
14
16
18
20
22
ROTATIONAL LEVEL

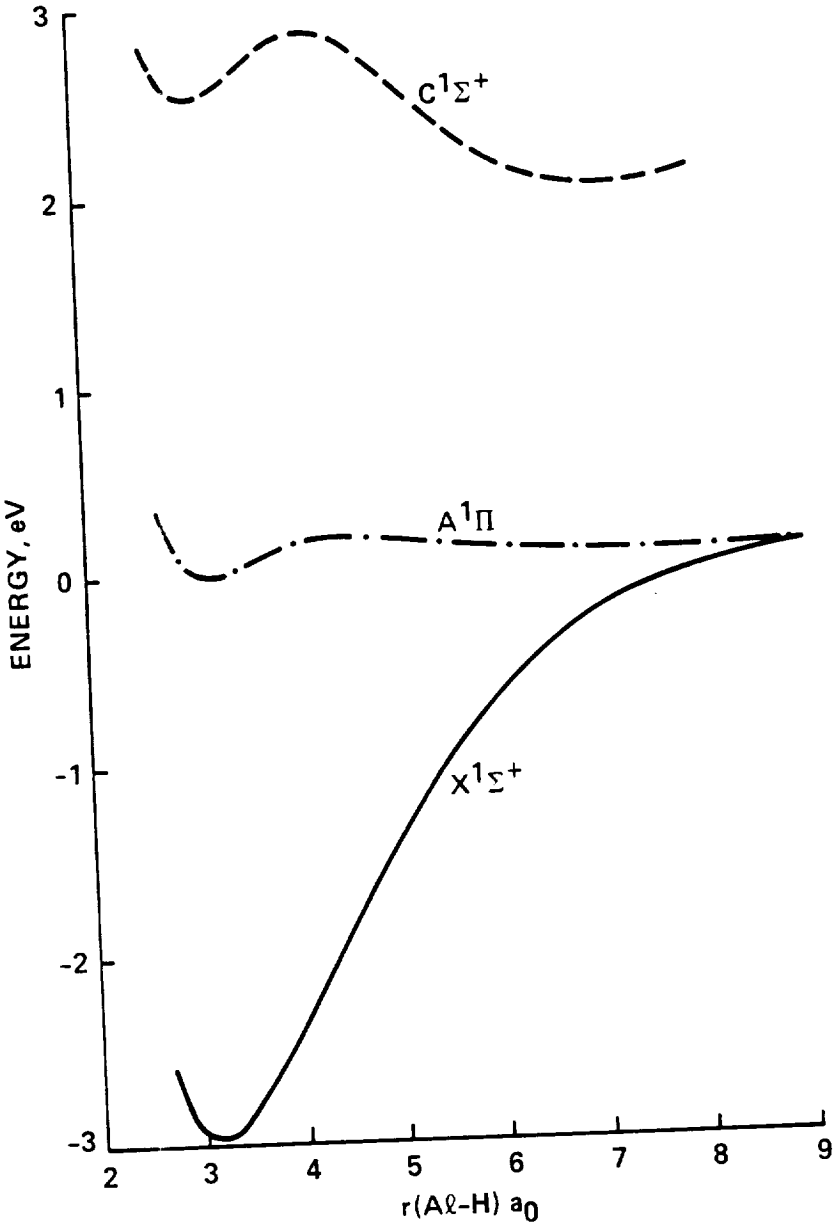
3
2
1
0
-1
-2
-3
ENERGY, eV
$C^1\Sigma^+$
$A^1\Pi$
$X^1\Sigma^+$
2
3
4
5
6
7
8
9
r(Aℓ-H) a_0
LANGHOFF

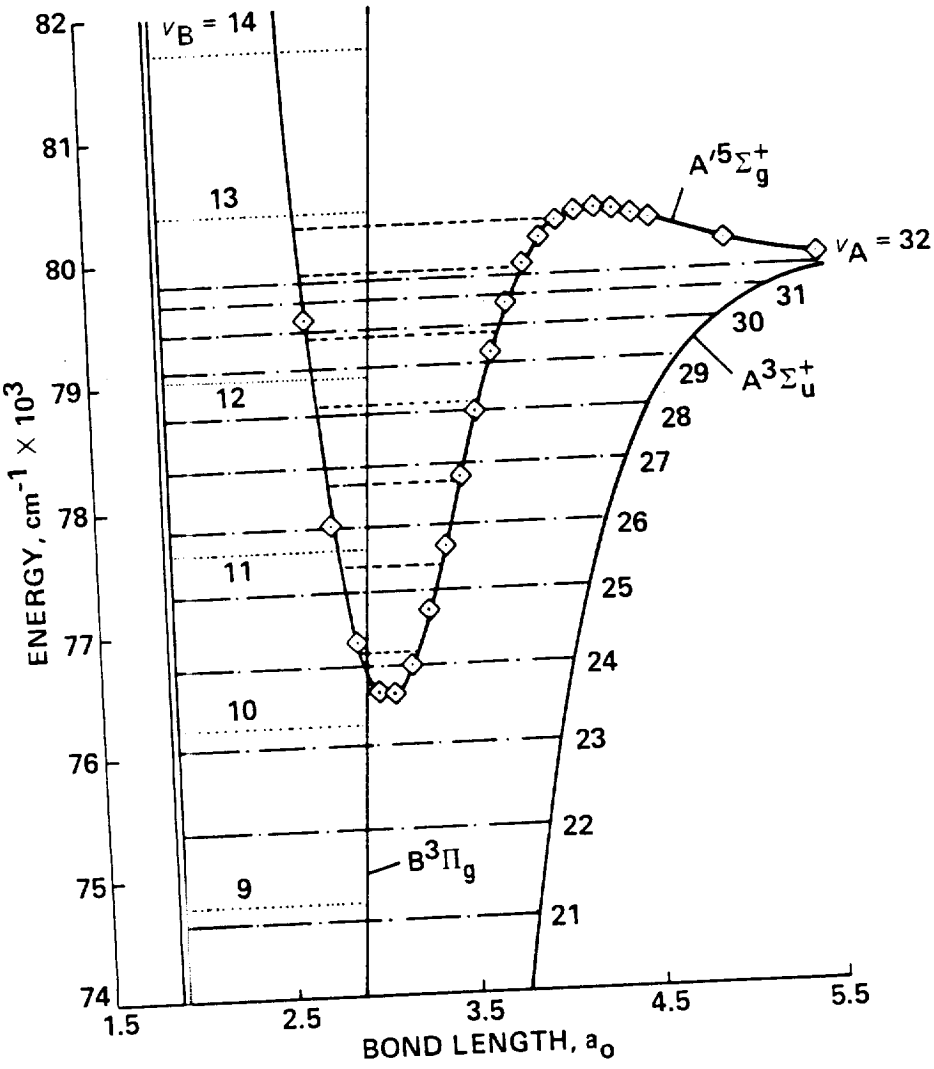
82
81
80
79
78
77
76
75
74
ENERGY, cm^{-1} × 10^3
v_B = 14
13
12
11
10
9
$A'^5\Sigma_g^+$
v_A = 32
31
30
29
$A^3\Sigma_u^+$
28
27
26
25
24
23
22
21
$B^3\Pi_g$
1.5
2.5
3.5
4.5
5.5
BOND LENGTH, a_o